

# Evidence of deep-water inflow in a tectonic window of the northern Apennines (Italy)

F. Cervi · L. Borgatti · G. Martinelli ·  
F. Ronchetti

Received: 27 July 2013 / Accepted: 14 February 2014  
© Springer-Verlag Berlin Heidelberg 2014

**Abstract** Water samples from the river network and from some shallow and brackish springs located in a tectonic window of the northern Apennines of Italy were studied in the frame of a comprehensive hydrogeological investigation in order to better understand the origin and the mixing processes between the two water types noticed also in previous studies (Ca–HCO<sub>3</sub> and Na–Cl). A sampling campaign covering the drought period during year 2010 was planned to gather electric conductivity, temperature and redox potential data along the river network and on groundwater occurrences located inside the tectonic structure. Additionally, eight water samples were collected for hydrochemical (major anions and cations: Na<sup>+</sup>, K<sup>+</sup>, Ca<sup>2+</sup>, Mg<sup>2+</sup>, HCO<sub>3</sub><sup>-</sup>, Cl<sup>-</sup>, SO<sub>4</sub><sup>2-</sup> and trace ion B<sub>tot</sub>) and isotopic ( $\delta^{18}\text{O}$ ,  $\delta^2\text{H}$ ,  $^3\text{H}$ ) analyses and compared with other eighteen samples from shallow and brackish springs collected near the study site during the period 2005–2012. Moreover, river discharge and water balance estimations were carried out. Results confirmed the presence of old Na–Cl water with salinity progressively increasing up to 5.5 g l<sup>-1</sup> at the northern termination of the tectonic window. These values

are in agreement with the ions contents of the most mineralized spring (Macognano spring: salinity of 7.6 g l<sup>-1</sup>), which has been considered as having the deepest and longest flow-path. Stable isotopes and trace ions contents are consistent with rainfall and snowmelt water mixed with brines associated with a hydrocarbon reservoir hosted at depth. Considering as end-member the more mineralized Na–Cl water, a cumulate inflow in the range of  $12.9 \pm 5.9 \text{ l s}^{-1}$  has been estimated. This aliquot is released into the river network with different mixing proportions by the groundwater occurrences discharging from the autochthonous flysch unit.

**Keywords** Hydrochemistry · Isotope geochemistry · Hydrogeology · Tectonic window · Northern Apennines · Italy

## Introduction

Hydrochemical and isotopic approaches have been widely used to depict groundwater origin (Kebede et al. 2010; Katsanou et al. 2012; Odeh et al. 2013), describe groundwater flow-paths (Johnson et al. 2012) and to quantify mixing processes between surface water and groundwater, occurring in different geological contexts (Gao et al. 2010; Guo et al. 2010; Petitta et al. 2011).

In the sedimentary fold-and-thrust belt of the northern Apennines of Italy, the presence of highly mineralized water (as high as 100 g l<sup>-1</sup>, i.e. brine water) has been recognized since long times (Camerana and Galdi 1911; Duchi et al. 2005). Different types of water are associated with CH<sub>4</sub>-degassing processes in compressive tectonic regimes (Tassi et al. 2012). In particular, they are commonly represented by water strongly enriched with sodium (up to 90 g l<sup>-1</sup>) and

---

F. Cervi (✉) · L. Borgatti  
DICAM, Department of Civil, Chemical, Environmental and  
Materials Engineering, ALMA MATER STUDIORUM  
University of Bologna, Viale Risorgimento, 2,  
41036 Bologna, Italy  
e-mail: federico.cervi2@unibo.it

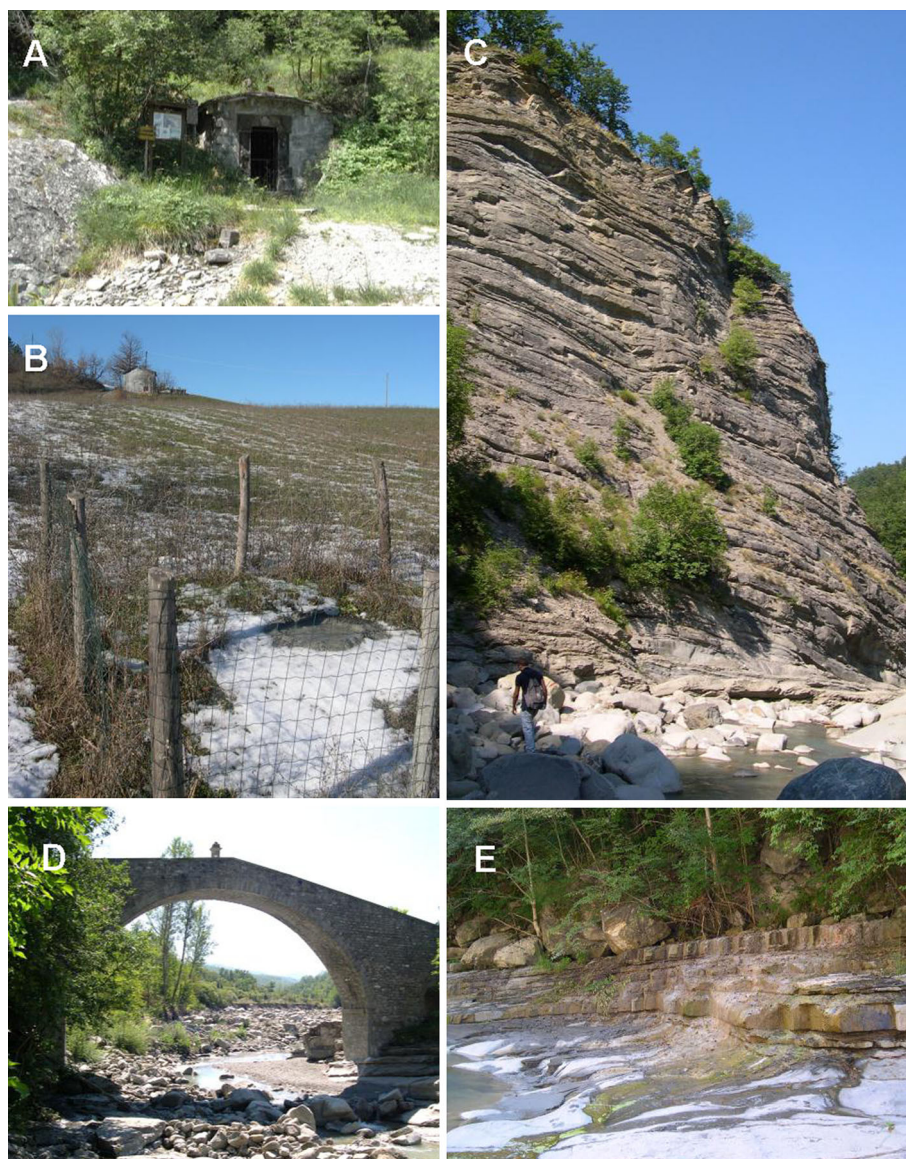
G. Martinelli  
ARPA Emilia-Romagna Sezione Provinciale di Reggio Emilia,  
Via Amendola, 2, 42122 Reggio, Italy

F. Ronchetti  
DSGC, Department of Chemical and Geological Sciences,  
University of Modena and Reggio Emilia, Largo S. Eufemia, 19,  
41121 Modena, Italy

chloride (up to  $50 \text{ g l}^{-1}$ ), together with some elements normally in-trace such as boron and strontium (Duchi et al. 2005; Boschetti et al. 2011), which can reach concentrations of several hundreds of  $\text{mg l}^{-1}$  (up to about 400 and  $550 \text{ mg l}^{-1}$ , respectively). The large part of this water is actually associated with mud volcanoes, which are widespread along the frontal part of the mountain chain, where poorly consolidated clay-rich units outcrop (Martinelli and Judd 2004). By taking origin from hydrocarbon reservoirs located at depth of more than 2,000 m, particles of clays and entrapped connate water of the old Pliocene sea are being flushed out and eventually reach the surface (Bonini 2007; Capozzi and Picotti 2010). These phenomena are related to the compressive field-stress characterizing the area (Capozzi and Picotti 2002). Some other occurrences of Na–Cl water are located in the inner sector of chain, where an extensional tectonic regime is currently developing (Minissale et al.

2000; Buttinelli et al. 2011; Bonini 2013). They consist of brackish springs (salinity up to  $20 \text{ g l}^{-1}$ ) with very low discharge ( $<1 \text{ l s}^{-1}$ ), flowing out from autochthonous sandstone units outcropping in some tectonic windows, whose burial history has been recently analysed by Botti et al. (2004): Bobbio (Boschetti et al. 2011; Trebbia River watershed), Porretta (Ciancabilla et al. 2007; Reno River), Miano (Duchi et al. 2005; Parma River), Salsominore (Boschetti et al. 2011; Stirone River), Vedriano (Bertolini and Gorgoni 2001; Enza River). In this context, water occurrences are never associated with mud volcano phenomena (Kopf 2002; Etiope and Martinelli 2009). These natural occurrences are related to low-temperature geothermal fields manifesting with water temperature between 19 and  $45 \text{ }^\circ\text{C}$  and local increase in geothermic gradient (RER 2010). Unfortunately, although they have been intensively exploited since ancient times, a detailed knowledge on the

**Fig. 1** Gova tectonic window study site. **a** The restored eighteen century hut of Quara Bath; inside the building Na–Cl water flow out from the outcropping bedrock with a discharge in the order of less than  $1 \text{ l min}^{-1}$  (BSQ, see Table 2). **b** The Macognano Na–Cl brackish spring, located some hundred metres downstream of Quara (BSM, see Table 2). **c** The thick turbiditic sequence of Gova sandstones in the middle part of the tectonic window; the total height of the gorge is in the order of 300 m. **d** The Medieval bridge of Cadignano that marks the northern initiation of the Gova tectonic window. **e** Outcrop of Gova sandstones along the Dolo River, where the network of mesostructures is visible given by the bedding and two joint sets. Na–Cl groundwater occurrences are mainly located along primary discontinuities. See Fig. 2 for the location of pictures



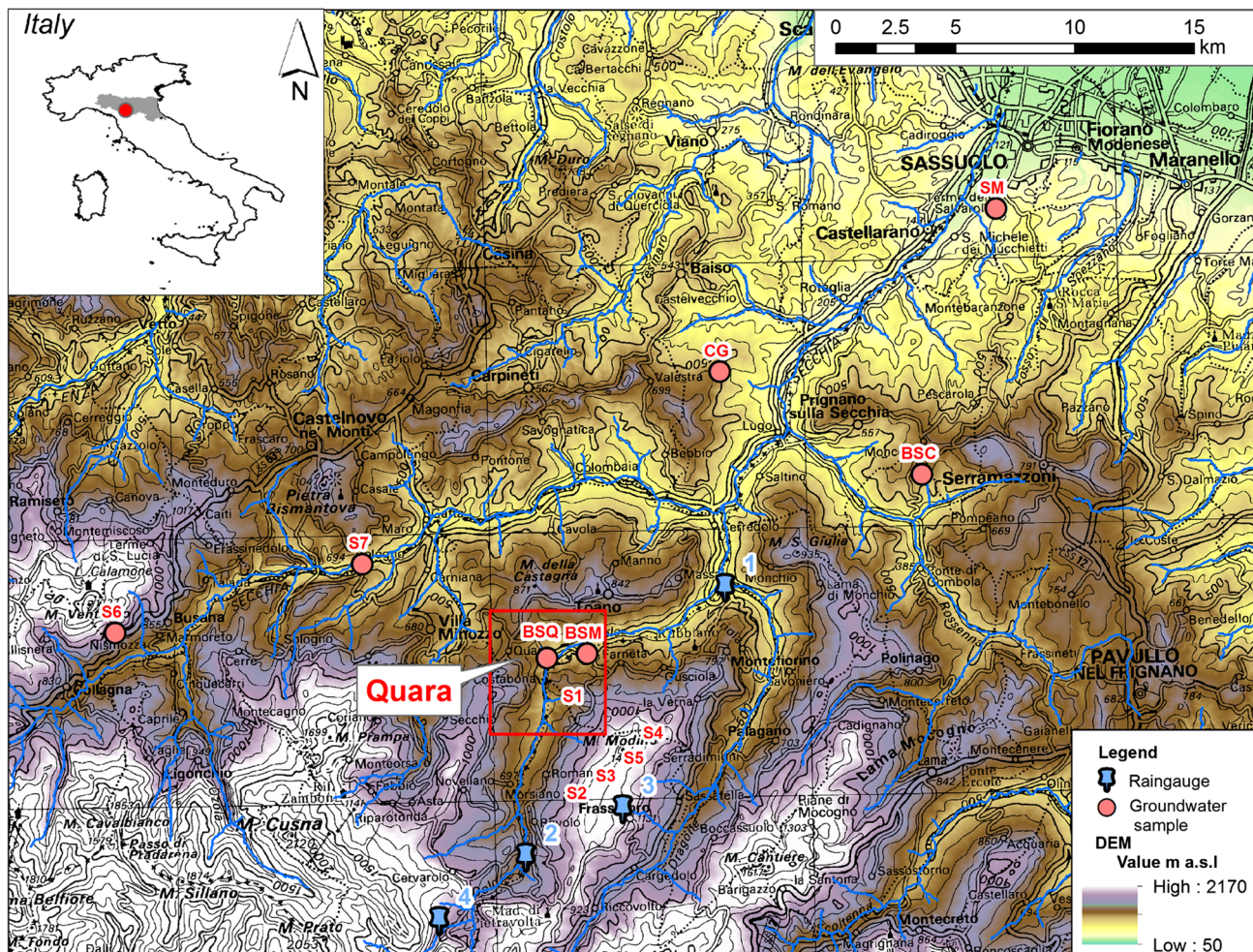


**Fig. 2** Ca–HCO<sub>3</sub> shallow springs (S1, S2, S3, S4, S5, S6, S7), Brackish Na–Cl springs (BSQ, BSM, BSC, CG) and mud volcano (SM) are shown (see Table 2 for details) together with raingauges (1,

2, 3, 4; see Table 1 for details). The tectonic window of Gova including the thermal area of Quara is identified by the red rectangle

origin and the mixing processes of this peculiar water has not been fully achieved to date.

The present study is focused on the thermal area of Quara (Reggio Emilia Province, Emilia-Romagna Region; Figs. 1, 2), which is located in the tectonic window of Gova, in the northern Apennines, along the Dolo River (Fig. 1d). Several springs and groundwater occurrences (Fig. 1a, e) discharge from the autochthonous turbiditic unit (Fig. 1c) outcropping close to a regional normal fault; seepage of highly mineralized water (associated with CH<sub>4</sub> degassing, Tassi et al. 2012) is also clearly visible as bubbling along the streambed that crosses the tectonic structure from N to S and as diffuse groundwater occurrences along the slopes (Fig. 1e). In the vicinity, the presence of the Macognano brackish spring is well known (Fig. 1b). Here, detailed hydrochemical and isotopic surveys were carried out in order to unravel the origin and the mixing processes of the Na–Cl water and for providing a conceptual hydrogeological model.

On the basis of temperature and pressure reached by the autochthonous units estimated by vitrinite reflectance analysis (Carlini et al. 2013), the boundary conditions for geochemical modelling were set and, together with the petrographic composition data, have allowed some conclusions to be drawn on the origin and evolution of the pore water interacting with the mineral assemblage of host rocks.

Moreover, the highly mineralized water aliquot rising into the streambed has been quantitatively assessed.

### Study area

#### Brief historical overview

As documented by Pliny the Elder in his *Historia Mundi Naturalis* (77–78 AD), Quara (Fig. 2) was an ancient and well-known Roman site called *Aquarium* (translation from

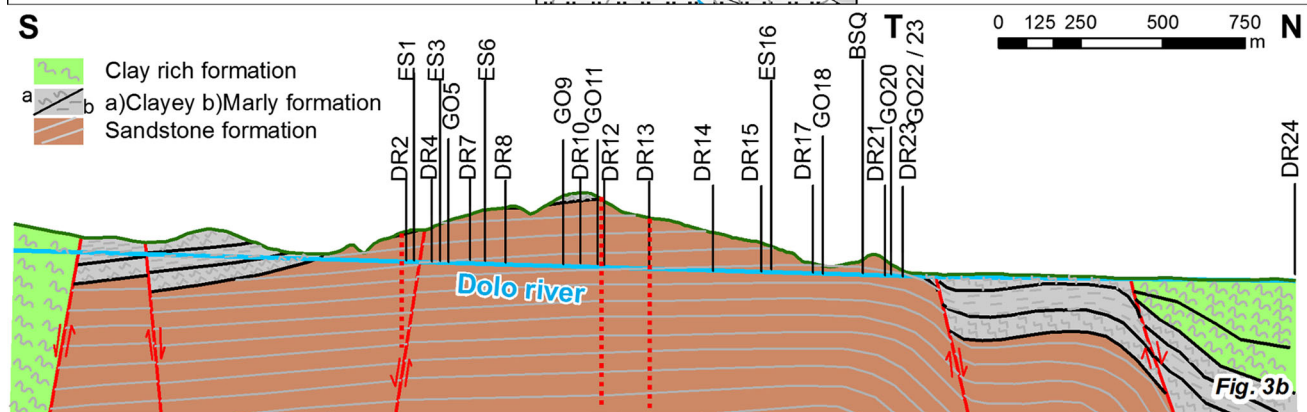
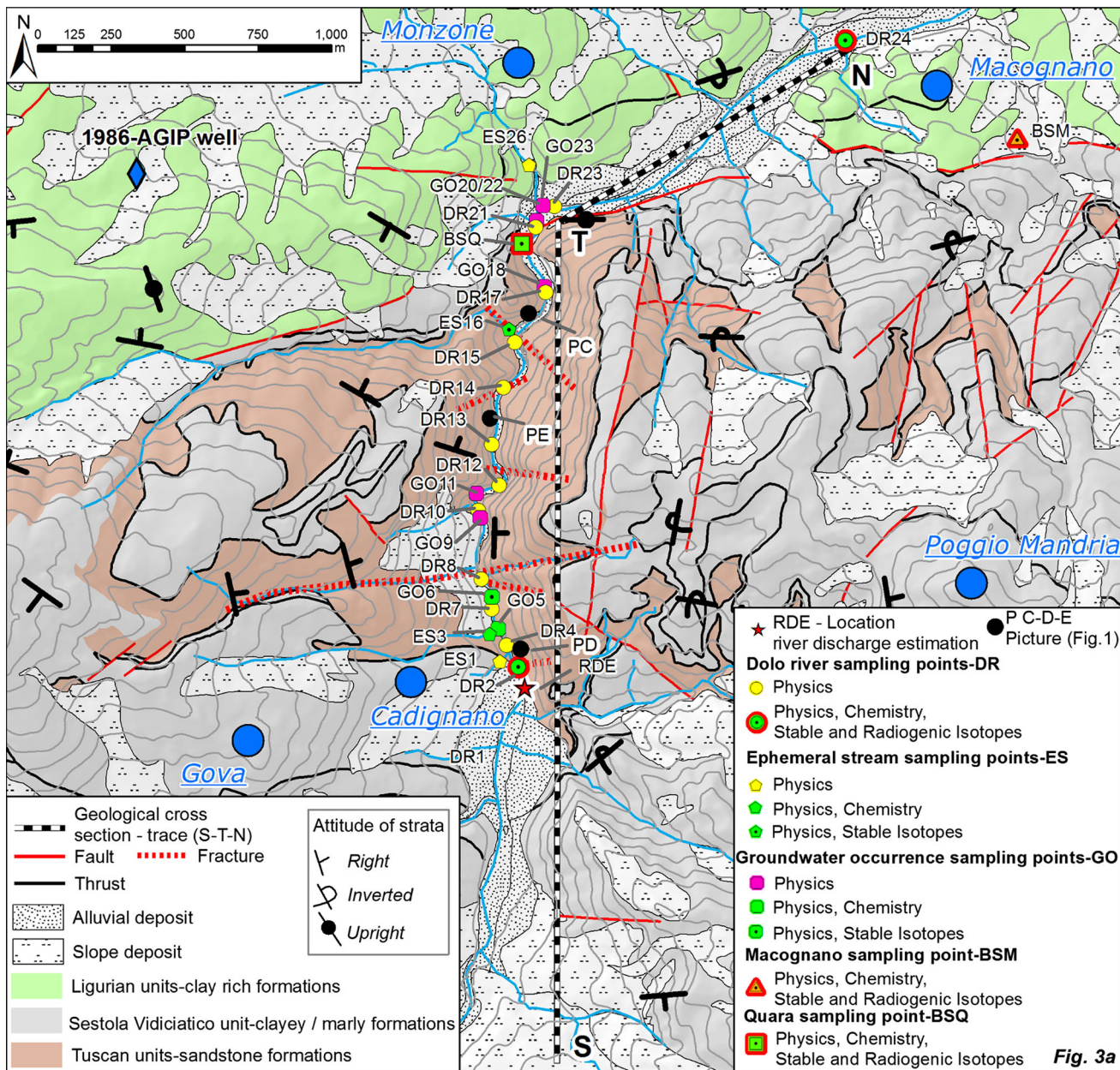


**Fig. 3** Gova study site. **a** Geological sketch map. The outcropping units are mapped together with structural and geomorphological features. The location of the 1986 AGIP exploration well is also reported. The trace of the geological cross-section is mapped (see Fig. 3). Salt slug-injection location for the river discharge estimation (RDE) is also shown, together with groundwater and superficial river network sampling locations. **b** S–N geological cross-section

Latin “bath”). To date, no ancient ruin is visible, except for some grooves in the rocks that served as support for the buildings. The recently restored eighteenth century hut is located on the roman ruins (Fig. 1a). The ancient *thermae* consisted of several connected tanks, which were used to collect the water flowing out at the bottom of the rock slope and then exploited for bathing and healing purposes. Several authors (Savonarola 1442; Biondi 1527; Alberti 1552; Bianchelli 1553; Bacci 1571) asserted the existence of pools even during the late Middle Ages and the beginning of Renaissance, confirming the importance of the site for therapeutic purposes. Their use is confirmed until the end of the eighteenth century (Vallisneri 1703; Ricci 1788), when the historical records began suddenly to be less continuous. Between the I and the II World Wars, water outflowing from several occurrences was used for salt production, but only at a local scale.

Recently, the area regained importance in the framework of a national project for oil and gas exploitation. Considering the presence of salt water as evidence of a deep hydrocarbon reservoir, a borehole of the total depth of 3,200 m investigated the geological structure (Fig. 3a); the well was drilled during year 1986 and the data are available on <http://unmig.sviluppoeconomico.gov.it/videpi/en/>. In detail, gas emissions (methane, nitrogen) were noticed at the mean depths of 1,800 and 2700 m, while no traces of oil and hydrocarbon were found. Gas emissions were accompanied by salt water (Na–Cl) with salinity up to 9 g l<sup>-1</sup>.

Geological and hydrogeological settings

The northern Apennines are a fold-and-thrust belt originated from the closure of the Ligure-Piemontese Ocean basin and the consequent collision between Adria and European continental plates (Boccaletti et al. 1971; Klingfield 1979; Molli 2008). This convergence has been responsible for the development of an accretionary prism made up of several tectono-stratigraphic units, which are separated by complex low-angle faults systems. In particular, Gova area is a part of a regional anticlinal structure, with a SW–NE trend (APAT 2002; Fig. 3b) where a thick

**Table 1** Effective rainfall calculated with Thornthwaite and Mather (1957) formula

Weather station	Code (as labelled in Fig. 2)	Year	Mean air temperature (°C)	Total rainfall (mm)	Total effective rainfall (mm)
Frassinoro	3	2006	9.7	834.2	380
Farneta	1		12.5	616	144
Fontanaluccia	2		9.8	1,103.0	543
Civago	4		9.5	1,385.6	751
Frassinoro	3	2007	10	837.8	275
Farneta	1		13.0	698.2	180
Fontanaluccia	2		10.7	1,009.8	468
Civago	4		9.9	1,423.8	825
Frassinoro	3	2008	9.6	1,248.4	805
Farneta	1		12.6	967.4	549
Fontanaluccia	2		9	1,562.8	1,214
Civago	4		9.4	2,434.2	1,963
Frassinoro	3	2009	9.7	1,313.5	807
Farneta	1		12.7	1,146.6	631
Fontanaluccia	2		10.7	1,756	1,302
Civago	4		9.6	2,564.0	2,016
Frassinoro	3	2010	8.4	1,439.8	780
Farneta	1		11.4	1,366.8	724
Fontanaluccia	2		9.6	2,022.6	1,297
Civago	4		8.4	2,790.8	2,131
Frassinoro	3	2011	9.6	765.6	361
Farneta	1		12.9	728.2	208
Fontanaluccia	2		11.4	957.4	638
Civago	4		9.9	1,520	1,019

**Table 2** Chemical (major and in-trace ions) and isotopic (stable and radiogenic) analyses

Sampling campaign	Name	COD	pH	T (°C)	Electrical conductivity 25 °C (µS cm <sup>-1</sup> )	PCO <sub>2</sub> (kPa)	Eh (mV)	Ca <sup>2+</sup> (mg l <sup>-1</sup> )	Mg <sup>2+</sup> (mg l <sup>-1</sup> )	Na <sup>+</sup> (mg l <sup>-1</sup> )	K <sup>+</sup> (mg l <sup>-1</sup> )	Sr <sup>2+</sup> (mg l <sup>-1</sup> )
22/06/2012	Macognano	B5Mb	7.8	21.2	12,430	n.a.	n.a.	n.a.	n.a.	n.a.	n.a.	n.a.
27/12/2011	Macognano	B5Ma	8.1	4.1	13,510	n.a.	n.a.	n.a.	n.a.	n.a.	n.a.	n.a.
26/08/2010	Dolo River	DR15	8.6	27.1	558	2.88	n.a.	35.8	8.6	65.0	3.3	n.a.
26/08/2010	Dolo River	DR24	8.5	28.1	640	3.69	n.a.	32.9	9.0	77.8	3.5	n.a.
26/08/2010	Dolo River	DR23	8.4	25.7	670	n.a.	n.a.	n.a.	n.a.	n.a.	n.a.	n.a.
26/08/2010	Dolo River	DR4	8.8	27.5	416	n.a.	106	n.a.	n.a.	n.a.	n.a.	n.a.
26/08/2010	Dolo River	DR7	8.6	27.1	426	n.a.	n.a.	n.a.	n.a.	n.a.	n.a.	n.a.
26/08/2010	Dolo River	DR8	8.7	27.2	443	n.a.	n.a.	n.a.	n.a.	n.a.	n.a.	n.a.
26/08/2010	Dolo River	DR10	8.6	26.9	457	n.a.	n.a.	n.a.	n.a.	n.a.	n.a.	n.a.
26/08/2010	Dolo River	DR12	8.5	27.3	546	n.a.	n.a.	n.a.	n.a.	n.a.	n.a.	n.a.
26/08/2010	Dolo River	DR13	8.6	27.2	507	n.a.	n.a.	n.a.	n.a.	n.a.	n.a.	n.a.
26/08/2010	Dolo River	DR14	8.6	26.7	530	n.a.	n.a.	n.a.	n.a.	n.a.	n.a.	n.a.
26/08/2010	Dolo River	DR17	8.4	27.9	570	n.a.	n.a.	n.a.	n.a.	n.a.	n.a.	n.a.
26/08/2010	Dolo River	DR21	8.4	25.7	670	n.a.	n.a.	n.a.	n.a.	n.a.	n.a.	n.a.
26/08/2010	Dolo River	DR2	8.5	27.4	406	3.56	82	34.8	8.2	38.5	2.6	n.a.
26/08/2010	Ephemeral stream	ES3	8.1	20.3	492	5.10	106	59.0	15.3	36.5	3.2	n.a.
26/08/2010	Ephemeral stream	ES16	8.5	20.4	392	3.59	n.a.	48.3	8.7	27.7	2.5	n.a.
26/08/2010	Ephemeral stream	ES1	8.2	19.4	521	n.a.	n.a.	n.a.	n.a.	n.a.	n.a.	n.a.
26/08/2010	Ephemeral stream	ES26	8.1	20.4	577	n.a.	n.a.	n.a.	n.a.	n.a.	n.a.	n.a.
26/08/2010	Quara	BSQa	7.7	19.4	14,520	4.65	n.a.	60.0	12.5	2,435.4	50.5	n.a.
26/08/2010	Groundwater occurrence	GO5	7.6	17.8	855	5.92	-90	91.1	17.3	55.5	5.1	n.a.
26/08/2010	Groundwater occurrence	GO6	8.3	17.2	3190	2.23	-253	42.2	6.1	578.3	10.6	n.a.
26/08/2010	Groundwater occurrence	GO9	8.4	19.8	2,370	n.a.	n.a.	n.a.	n.a.	n.a.	n.a.	n.a.
26/08/2010	Groundwater occurrence	GO11	8.2	19.7	1,542	n.a.	n.a.	n.a.	n.a.	n.a.	n.a.	n.a.
26/08/2010	Groundwater occurrence	GO18	8.1	23.1	7,570	n.a.	-190	n.a.	n.a.	n.a.	n.a.	n.a.
26/08/2010	Groundwater occurrence	GO20	7.8	21.1	1,910	n.a.	n.a.	n.a.	n.a.	n.a.	n.a.	n.a.
26/08/2010	Groundwater occurrence	GO22	7.9	22.9	1,104	n.a.	n.a.	n.a.	n.a.	n.a.	n.a.	n.a.

Table 2 continued

COD	B <sub>tot</sub> (mg l <sup>-1</sup> )	HCO <sub>3</sub> <sup>-</sup> (mg l <sup>-1</sup> )	Cl <sup>-</sup> (mg l <sup>-1</sup> )	SO <sub>4</sub> <sup>2-</sup> (mg l <sup>-1</sup> )	δ <sup>2</sup> H (‰)	δ <sup>18</sup> O (‰)	Tritium (TU)					
BSMb	28.3	n.a.	n.a.	n.a.	-38.52	-3.68	n.a.					
BSMa	n.a.	n.a.	n.a.	n.a.	-41.01	-4.10	0.0					
DR15	n.a.	229.0	51.9	8.6	n.a.	n.a.	n.a.					
DR24	n.a.	217.0	73.7	10.0	-56.65	-8.48	6.3					
DR23	n.a.	n.a.	n.a.	n.a.	n.a.	n.a.	n.a.					
DR4	n.a.	n.a.	n.a.	n.a.	n.a.	n.a.	n.a.					
DR7	n.a.	n.a.	n.a.	n.a.	n.a.	n.a.	n.a.					
DR8	n.a.	n.a.	n.a.	n.a.	n.a.	n.a.	n.a.					
DR10	n.a.	n.a.	n.a.	n.a.	n.a.	n.a.	n.a.					
DR12	n.a.	n.a.	n.a.	n.a.	n.a.	n.a.	n.a.					
DR13	n.a.	n.a.	n.a.	n.a.	n.a.	n.a.	n.a.					
DR14	n.a.	n.a.	n.a.	n.a.	n.a.	n.a.	n.a.					
DR17	n.a.	n.a.	n.a.	n.a.	n.a.	n.a.	n.a.					
DR21	n.a.	n.a.	n.a.	n.a.	n.a.	n.a.	n.a.					
DR2	n.a.	199.0	24.2	9.4	-57.27	-8.42	5.8					
ES3	n.a.	282.0	35.6	10.3	n.a.	n.a.	n.a.					
ES16	n.a.	205.0	31.8	5.1	-59.78	-9.06	n.a.					
ES1	n.a.	n.a.	n.a.	n.a.	n.a.	n.a.	n.a.					
ES26	n.a.	n.a.	n.a.	n.a.	n.a.	n.a.	n.a.					
BSQa	n.a.	1,204.0	3,243.9	0.5	-59.74	-8.70	0.7					
GO5	n.a.	398.0	63.3	9.7	n.a.	n.a.	n.a.					
GO6	n.a.	410.0	750.4	4.6	-62.41	-9.05	n.a.					
GO9	n.a.	n.a.	n.a.	n.a.	n.a.	n.a.	n.a.					
GO11	n.a.	n.a.	n.a.	n.a.	n.a.	n.a.	n.a.					
GO18	n.a.	n.a.	n.a.	n.a.	n.a.	n.a.	n.a.					
GO20	n.a.	n.a.	n.a.	n.a.	n.a.	n.a.	n.a.					
GO22	n.a.	n.a.	n.a.	n.a.	n.a.	n.a.	n.a.					
Sampling campaign	Name	COD	pH	T (°C)	Electrical conductivity 25 °C (µS cm <sup>-1</sup> )	PCO <sub>2</sub> (kPa)	Eh (mV)	Ca <sup>2+</sup> (mg l <sup>-1</sup> )	Mg <sup>2+</sup> (mg l <sup>-1</sup> )	Na <sup>+</sup> (mg l <sup>-1</sup> )	K <sup>+</sup> (mg l <sup>-1</sup> )	SP <sup>2+</sup> (mg l <sup>-1</sup> )
26/08/2,010	Groundwater occurrence	GO23	7.8	22.7	1010	n.a.	n.a.	n.a.	n.a.	n.a.	n.a.	n.a.
27/09/2013	Canalina	BSC	n.a.	n.a.	14,900	n.a.	n.a.	79.0	85.3	n.a.	5.2	10.5
27/05/2008	Pian di Venano	S2a	n.a.	n.a.	n.a.	n.a.	n.a.	n.a.	n.a.	n.a.	n.a.	n.a.
22/11/2,007	Are Vecchie	S3a	n.a.	n.a.	n.a.	n.a.	n.a.	n.a.	n.a.	n.a.	n.a.	n.a.
22/11/2007	Riva	S1a	n.a.	n.a.	n.a.	n.a.	n.a.	n.a.	n.a.	n.a.	n.a.	n.a.

**Table 2** continued

Sampling campaign	Name	COD	pH	T (°C)	Electrical conductivity 25 °C (µS cm <sup>-1</sup> )	PCO <sub>2</sub> (kPa)	Eh (mV)	Ca <sup>2+</sup> (mg l <sup>-1</sup> )	Mg <sup>2+</sup> (mg l <sup>-1</sup> )	Na <sup>+</sup> (mg l <sup>-1</sup> )	K <sup>+</sup> (mg l <sup>-1</sup> )	SR <sup>2+</sup> (mg l <sup>-1</sup> )
22/11/2007	Venano	S5a	7.4	10.4	164	n.a.	n.a.	n.a.	n.a.	n.a.	n.a.	n.a.
20/11/2007	Pian di Venano	S2b	n.a.	n.a.	n.a.	n.a.	n.a.	n.a.	n.a.	n.a.	n.a.	n.a.
18/07/2007	Are Vecchie	S3b	7.7	10.7	550	1.81	n.a.	60.0	14.7	30.0	4.5	n.a.
18/07/2007	Lago verde	S4a	7.9	7.0	210	1.49	n.a.	35.2	7.0	9.0	2.0	n.a.
18/07/2007	Pian di Venano	S2c	7.8	9.5	360	1.87	n.a.	62.3	10.0	16.0	1.0	n.a.
18/07/2007	Riva	S1b	7.3	11.9	650	n.a.	n.a.	n.a.	n.a.	n.a.	n.a.	n.a.
18/07/2007	Venano	S5b	7.4	10.4	164	n.a.	n.a.	n.a.	n.a.	n.a.	n.a.	n.a.
27/07/2005	Pian di Venano	S2d	7.1	11.2	371	n.a.	n.a.	n.a.	n.a.	n.a.	n.a.	n.a.
27/07/2005	Venano	S5c	7.4	10.4	164	n.a.	n.a.	n.a.	n.a.	n.a.	n.a.	n.a.
26/07/2005	Lago Verde	S4b	n.a.	n.a.	n.a.	n.a.	n.a.	n.a.	n.a.	n.a.	n.a.	n.a.
18/03/2005	Venano	S5d	n.a.	n.a.	n.a.	n.a.	n.a.	n.a.	n.a.	n.a.	n.a.	n.a.
22/02/2005	Lago Verde	S4c	7.7	8.0	157	n.a.	n.a.	n.a.	n.a.	n.a.	n.a.	n.a.
Cervi et al. (2012)	Ca' Lita	CGa	7.4	n.a.	7,577	4.10	n.a.	146.0	67.0	1,660.0	22.0	6.8
Cervi et al. (2012)	Ca' Lita	CGb	7.6	n.a.	5,088	4.70	n.a.	7.9	6.2	1,155.0	3.0	n.a.
Colombetti and Nicolodi (2005)	Macognano	BSMc	8.7	n.a.	14,730	n.a.	n.a.	44.6	55.8	3,100.0	38.0	11.5
Cervi et al. (2012)	Nismozza	S6	7.8	n.a.	274	1.50	n.a.	41.0	6.0	13.0	1.1	0.6
Cervi et al. (2012)	Poiano	S7	7.6	n.a.	11,093	n.a.	n.a.	788.0	43.0	1,750.0	13.0	10.2
Boschetti et al. (2011)	Quara	BSQb	7.3	n.a.	10,200	n.a.	n.a.	32.0	8.3	2,559.0	57.0	6.2
Boschetti et al. (2011)	Salvarola mud volcano	SM	8.2	n.a.	24,484	n.a.	n.a.	7.0	17.0	6,670.0	28.0	4.6
COD	B <sub>tot</sub> (mg l <sup>-1</sup> )	HCO <sub>3</sub> <sup>3-</sup> (mg l <sup>-1</sup> )	Cl <sup>-</sup> (mg l <sup>-1</sup> )	SO <sub>4</sub> <sup>2-</sup> (mg l <sup>-1</sup> )	δ <sup>2</sup> H (‰)	δ <sup>18</sup> O (‰)	Tritium (TU)					
GO23	n.a.	n.a.	n.a.	n.a.	n.a.	n.a.	n.a.					
BSC	16.0	n.a.	4,821.0	5.0	n.a.	n.a.	n.a.					
S2a	n.a.	n.a.	n.a.	n.a.	-66.46	-9.89	n.a.					
S3a	n.a.	n.a.	n.a.	n.a.	-67.94	-10.14	n.a.					
S1a	n.a.	n.a.	n.a.	n.a.	-69.27	-9.79	n.a.					
S5a	n.a.	n.a.	n.a.	n.a.	-70.15	-10.20	n.a.					
S2b	n.a.	n.a.	n.a.	n.a.	-66.46	-9.89	n.a.					
S3b	n.a.	261.0	3.8	68.0	-69.37	-9.77	n.a.					
S4a	n.a.	140.0	3.1	19.0	-68.59	-9.91	n.a.					
S2c	n.a.	240.0	5.1	28.0	-66.18	-9.67	n.a.					
S1b	n.a.	n.a.	n.a.	n.a.	-66.18	-9.31	n.a.					
S5b	n.a.	n.a.	n.a.	n.a.	-67.87	-9.91	n.a.					
S2d	n.a.	n.a.	n.a.	n.a.	-69.10	-9.48	n.a.					
S5c	n.a.	n.a.	n.a.	n.a.	-67.26	-10.22	n.a.					

Table 2 continued

COD	B <sub>tot</sub> (mg l <sup>-1</sup> )	HCO <sub>3</sub> <sup>3-</sup> (mg l <sup>-1</sup> )	Cl <sup>-</sup> (mg l <sup>-1</sup> )	SO <sub>4</sub> <sup>2-</sup> (mg l <sup>-1</sup> )	δ <sup>2</sup> H (‰)	δ <sup>18</sup> O (‰)	Tritium (TU)
S4b	n.a.	n.a.	n.a.	n.a.	-65.57	-9.88	n.a.
S5d	n.a.	n.a.	n.a.	n.a.	-69.90	-10.19	n.a.
S4c	n.a.	n.a.	n.a.	n.a.	-69.26	-10.44	n.a.
CGa	8.2	529.0	416.0	3,130.0	-52.38	-6.80	n.a.
CGb	n.a.	525.0	787.0	980.0	-49.23	-5.33	n.a.
BSMc	n.a.	1,121.0	4,634.0	2.2	n.a.	n.a.	n.a.
S6	0.0	152.0	5.0	31.0	n.a.	-9.17	n.a.
S7	0.1	168.0	3,405.0	2,045.0	n.a.	-8.94	n.a.
BSQb	8.9	776.0	4,059.0	n.a.	-59.40	-8.56	n.a.
SM	121.0	2,130.0	10,190.0	4.0	-13.50	4.00	n.a.

Samples from river network, Na-Cl groundwater occurrences, Quara and Macognano, and Ca-HCO<sub>3</sub> shallow springs. Other samples are reported for further comparison: Salvarola mud volcano (Boschetti et al. 2011), Ca' Lita (Cervi et al. 2012) and Canalina brackish water and Poiano evaporites-related spring (Cervi 2003)

foredeep turbidite sequence (Gova sandstones, Langhian, lower Miocene; Plesi 2002) belonging to the Tuscan Unit was overthrust by highly tectonized Ligurian marly and clayey shale rocks (Sestola-Vidiciatico unit, Cretaceous—middle Eocene). Northward, a NW–SE dipping high-angle normal fault lowered the multi layered pelagic clayey units and calcareous-arenaceous turbidites (Ligurian units, Late Cretaceous—Early Tertiary) exhuming the buried foredeep units, with a vertical throw of more than 3 km (Remitti et al. 2012). These tectonic stresses result in three joint sets visible at the mesoscale (Fig. 1e; Remitti et al. 2012). Recently, by considering vitrinite reflectance on the dispersed organic matter and mineralogical analyses on the clayey fraction contained in several samples from the Gova sandstones, Carlini et al. (2013) suggested a burial of this formation at depth of about 4–4.5 km, which took place after the deposition. The same Authors provided the maximum temperature and pressure reached: 110–140 °C and about 42–52.5 Mpa, respectively.

The Dolo River crosses the tectonic structure from south to north; in the southern part of the tectonic window (i.e. at its initiation), intensive fluvial erosion processes developing in the Gova sandstones have produced a steep canyon, more than 300 m deep (Fig. 1c). In the northern part, alluvial deposits with a thickness of 10 m cover the underlying bedrock (APAT 2002). Two ephemeral streams are located in the left-hand sector of the catchment (Fig. 3a). Because of the outcropping lithologies, rivers and streams display highly variable discharges, with drought occurring during dry periods.

The area is characterized by an annual rainfall of about 800–1,300 mm, distributed between October and May (30-years record from the Frassinoro weather station: 3 km south-eastward, elevation of 1,122 m a.s.l.; Fig. 2). Snowmelt is extremely variable from year to year but it can account even for 200–400 mm of equivalent rainfall, leading to a total precipitation of more than 1,500 mm. Effective rainfall has been estimated using the Thornthwaite and Mather (1957) formula (Table 1) for the period 2006–2011 by considering also further three weather stations located in the Dolo catchment (Farneta, 3 km north-eastward, 380 m a.s.l.; Fontanaluccia, 9 km southward, 787 m a.s.l.; Civago, 12 km southward, 1,051 m a.s.l.). With a mean annual air temperature between 8.4 and 13.0 °C, a water surplus ranging from 100 to 700 mm/year was available in the tectonic window (elevation from 500 to 900 m a.s.l.) and could be supplied to the soil between November and April.

Due to the high content of clayey sediments in the matrix, the geological units outcropping in northern Apennines are generally characterized by low permeability and low storage coefficients (Corsini et al. 2009); consequently, shallow springs (Ca-HCO<sub>3</sub>) present peak

discharges which are directly linked to the most intense precipitations and can even disappear during dry periods (Cremaschi 2008).

In the Gova tectonic window, beside shallow springs, some Na–Cl groundwater occurrences can be found, i.e. brackish springs flowing out from the autochthonous flysch and from the clay-rich units (Table 2 and Fig. 3a). All these groundwater occurrences display very low and almost constant discharge during the year ( $<1 \text{ l min}^{-1}$ ).

## Methods

The study consisted of hydrological, hydrochemical and isotopic surveys which were carried out on superficial water and on groundwater samples collected during summer 2010 along the tectonic window of Gova, from the brackish and shallow springs flowing out from the surrounding slopes. More specifically, the water–groundwater chemistry and the stable isotope contents were estimated in order to characterize end-members origin and eventual mixing phenomena. By collecting local springs water, the reference isotopic value ( $\delta^{18}\text{O}$ ) for rainfall recharge water was defined and then assumed as input in the estimated infiltration through the Gova flysch rock mass.

An independent validation, to check if the peculiar water chemistry could be eventually due only to the mineralogical composition of the Gova flysch rock, consisted in an equilibrium-based model that took into account the long-term chemical interaction between pore water solutions and host rocks.

The aliquot of deep Na–Cl water was estimated by coupling radioactive isotopes content ( $^3\text{H}$ ) with river discharge in the southern sector of the tectonic window. The

study was conducted during a period of minimum discharge (low flow) in the Dolo River, in order to enhance the contribution of the Na–Cl water into the streambed and to reduce the errors in the calculation of the corresponding aliquot.

Field surveys: water sampling and physical parameters assessment, river discharge assessment

Electric conductivity (EC), temperature (t) and acid potential (pH) were determined using a Hanna HI98130 tester, while redox potential (Eh) has been assessed with a Hanna HI98201 electrode. The same physical and chemical parameters were checked using a Crison MM40+ multimeter equipped with a Ross glass electrode for pH and Eh. Depending on the instrument, precisions are  $\pm 0.5\text{--}2\%$  (EC),  $\pm 0.2\text{--}0.5\text{ }^\circ\text{C}$  (t),  $\pm 0.01\text{--}0.05$  (pH) and  $\pm 1\text{--}5$  mV (Eh).

Total alkalinity was determined in the field by acidimetric titration and successively checked in laboratory by Gran titration (Gran 1952) not later than 24 h after sampling.

Water samples for laboratory analyses were filtered through  $0.45\text{-}\mu\text{m}$  cellulose membranes, and the aliquot for cation analysis was acidified with 65 %  $\text{HNO}_3$  Suprapur Merck.

River discharge was estimated by means of salt dilution method (Rantz et al. 1982). According to Tazioli (2011a, b), a hyper-concentrated solution was firstly prepared by diluting 0.5 kg of NaCl in 5 l of water and successively injected instantly (slug injection) into the river. Conductivity was measured in-continuous by means of an electric transducer equipped with conductivity probe (STS DL/70/ N MULTI); the acquisition time was set at 6 s. To ensure a

**Table 3** Mineralogical data input of the long-term interaction modelling between pore water and host rocks performed with the software PHREEQC

Phase	Molecular formula	Molecular weight	Simulation 1 % rock	Simulation 2 % rock	Simulation 1		Simulation 2	
					Grams	Moles	Grams	Moles
Quartz	$\text{SiO}_2$	60.08	63.45	72.8	11,507	189.26	5,918	98.51
K-feldspar	$\text{KAlSi}_3\text{O}_8$	278.36	2.64	3.04	478	1.72	247	0.89
Albite	$\text{NaAlSi}_3\text{O}_8$	262.27	7.911	9.12	1,140	1.82	1,236	2.83
Anorthite	$\text{CaAl}_2\text{Si}_2\text{O}_8$	278.26	2.64	3.04	478	5.17	247	0.89
Illite	$\text{K}_{0.6}\text{Mg}_{0.25}\text{Al}_{2.3}\text{Si}_{3.5}\text{O}_{10}(\text{OH})_2$	384	1.295	1.5	235	0.61	122	0.32
Ca-Montmorillonite (Smectite)	$\text{Ca}_{0.165}\text{Al}_{2.33}\text{Si}_{3.67}\text{O}_{10}(\text{OH})_2$	367	1.295	1.5	235	0.64	122	0.33
Chlorite	$\text{Mg}_5\text{Al}_2\text{Si}_3\text{O}_{10}(\text{OH})_8$	611.6	9.09	3	1,649	2.70	244	0.44
Hematite	$\text{Fe}_2\text{O}_3$	159.68	1.295	1.5	235	1.47	122	0.76
Muscovite	$\text{KAl}_3\text{Si}_3\text{O}_{10}(\text{OH})_{1.8}\text{F}_{0.2}$	398.76	2.59	3	470	1.18	244	0.61
Epidote	$\text{Ca}_2\text{Fe}_{2.25}\text{Al}_{0.75}(\text{SiO}_4)_3\text{OH}$	509.32	1.295	1.5	235	0.45	122	0.24
Calcite	$\text{CaCO}_3$	95.08	6.5	/	1,179	12.40	/	/

**Table 4** Data and results of the isotopic Ca–HCO<sub>3</sub>–Na–Cl water balance

Details	Source	Value	Precision
Data			
3H <sub>a</sub> Dolo River at the beginning of the tectonic window (related to discharge Q <sub>a</sub> and DR2 in Table 2)	Measured value	6.3 TU	±0.1 TU
3H <sub>b</sub> Na–Cl water end-member (related to discharge Q <sub>b</sub> and BSMc in Table 2)	Measured value	0.0 TU	±0.1 TU
3H <sub>c</sub> Dolo River at the end of the tectonic window (related to discharge Q <sub>c</sub> and DR24 in Table 2)	Measured value	5.8 TU	±0.1 TU
Q <sub>a</sub> Dolo River discharge at the beginning of the tectonic window	Measured value	150 l s <sup>-1</sup>	±6 l s <sup>-1</sup>
Results			
Q <sub>b</sub> Na–Cl water end-member discharge through the tectonic window	Eq. (2)	12.9 l s <sup>-1</sup>	±5.9 l s <sup>-1</sup>

Precision of tritium measured values is that of the analytical determination methods (Scintillation counting). Uncertainties in the final calculated value are assessed using error propagation methods presented by Taylor (1997). The uncertainty related to Q<sub>a</sub> is considered equal to ±4 % by Day (1976, 1977)

complete lateral homogenization, the probe was located in a river-flow constriction; the tracer has been instantaneously injected upstream at a distance well over the so-called good-mixing length (Tazioli 2011a, b). In this sector of the river, no pools or backwater areas were present (RDE point in Fig. 3a). In addition, the river streambed was characterized by the complete absence of alluvial deposits; therefore, no subsurface seepage could be possible. As reported by Day (1976, 1977), precisions are to be expected in the order of 4–7 %.

Laboratory analyses: chemical, water isotopes and tritium analyses

Major ion contents (Na<sup>+</sup>, K<sup>+</sup>, Ca<sup>2+</sup>, Mg<sup>2+</sup>, Cl<sup>-</sup>, SO<sub>4</sub><sup>2-</sup>) have been assessed using high-performance liquid chromatography while B<sub>tot</sub> by inductively coupled plasma optical emission spectrometry (ICP-OES). Ion Cl<sup>-</sup> was further controlled applying Mohr’s method. Data are reported in mg l<sup>-1</sup> (Table 2). The total relative uncertainty is <5 % for all compounds.

Stable oxygen and hydrogen isotope analyses (δ<sup>18</sup>O, δ<sup>2</sup>H, Table 2) were analysed by isotope ratio mass

spectrometry, in which the difference between the sample and the standard (Vienna Standard Mean Oceanic Water VSMOW) is determined. This deviation is presented in the standard δ-notation as per mil (‰) where  $\delta = [(R_S/R_{SMOW}) - 1] \times 1,000$ ; R<sub>S</sub> represents either the <sup>18</sup>O/<sup>16</sup>O or the <sup>2</sup>H/<sup>1</sup>H ratio of the sample, and R<sub>SMOW</sub> is <sup>18</sup>O/<sup>16</sup>O or the <sup>2</sup>H/<sup>1</sup>H ratio of the SMOW. The precisions are in the order of ±0.05 ‰ (δ<sup>18</sup>O) and ±0.70 ‰ (δ<sup>2</sup>H).

Isotope <sup>3</sup>H has been analysed by electrolytic enrichment and liquid scintillation counting method (Tazioli and Tazioli 2005, Theodorsson 1999). Results are presented as tritium unit (TU), in which one TU equals one tritium atom per 10<sup>18</sup> hydrogen atoms. Analytical errors are in the order of ±0.1 TU.

PHREEQC modelling: thermodynamic calculation and equilibrium-based approach

Mineral saturation indices and distribution of dissolved species (CO<sub>2</sub>) of water samples were calculated using PHREEQC software (Parkhurst and Appelo 1999) coupled with Lawrence Livermore National Laboratory thermodynamic database (LLNL database *llnl.dat*).

The same software was used for simulating the long-term interaction between an aqueous solution and the mineral assemblage of the rocks. Precipitation and dissolution of phases until equilibrium is reached were modelled starting from the mean rock composition of the Gova sandstones and reference rainfall and sea water chemical contents (as reported in section “Methods”).

More in details, in Simulation 1, only the flysch rock post-exhumation interaction was considered, and the starting solution was set equal to rainfall. In Simulation 2, the burial process was taken into account; therefore, pores were considered to be initially permeated by sea water. Furthermore, the progressive growth of pressure and temperature was simulated with a step by step procedure, until both reached the maximum values proposed by Carlini et al. (2013); due to the long time taken by this sedimentary and tectonic evolution, for each step represented by fixed values of temperature and pressure, equilibrium between solid assemblage and pore water has been achieved.

Ancient sea water chemical content was considered equal to the present-day Atlantic sea water composition (Nordstrom et al. 1979), while rainfall water ions were set equal to those reported by Panettiere et al. (2000).

The knowledge of the porosity is required for calculating the exact amounts of phases, which have interacted with the rock through the pores. According to the mean porosities reported by Freeze and Cherry (1979) for unconsolidated sediments and rocks, a mean porosity of 25 % has been taken into account for Simulation 2, while a slightly lower one (13 %) for simulation 1.

As reported in APAT (2002) and Valloni et al. (2002), the Gova flysch is composed by quartz (50.5 %), feldspar (10.6 %) and lithoidic fragments of different genesis (25.9 %) with a calcitic and phyllosilicatic (chlorite) secondary cement (13 %). Among the lithoids, metamorphic rocks are prevailing over those with a sedimentary origin (70.6 and 14.9 %, respectively) and are mainly made up of quartz, muscovite, chlorite, plagioclase, hematite and phyllosilicates such as illite and montmorillonite.

By considering a mean porosity of 13 and 25 %, respectively, the equivalent moles of each phase can be obtained and the values are reported in Table 3. It must be stressed that in Simulation 1, secondary cement was inserted in the mineralogical assemblage; on the contrary, Simulation 2 started with the primary bulk composition. Being precipitated during the diagenetic process, the secondary cement phases (calcite and chlorite) have been used as a further check within the solid phases which were progressively removed from the pore solution during the simulation. Additional thermodynamic data of the minerals used for simulations come from THERMODDEM website (epidote and muscovite, <http://thermoddem.brgm.fr>).

#### Hydrological water balance

The deep-water inflow was estimated by solving a simplified discharge-balance equation and by processing the  $^3\text{H}$  data as

described by Mazor (1997). In particular, considering the river discharge at the northern termination of the tectonic window ( $Q_c$ ) as only composed by the sum of the two aliquots  $Q_a$  (river discharge at the beginning of the tectonic window) and  $Q_b$  (Na–Cl water), the following formula can be written:

$$Q_a \cdot {}^3\text{H}_a + Q_b \cdot {}^3\text{H}_b = Q_c \cdot {}^3\text{H}_c \quad (1)$$

where,  ${}^3\text{H}_a$ ,  ${}^3\text{H}_b$  and  ${}^3\text{H}_c$  are the corresponding tritium contents of the three different aliquots.

Considering that  $Q_a + Q_b = Q_c$ ,  $Q_b$  can be obtained by:

$$Q_b = Q_a \cdot ({}^3\text{H}_a - {}^3\text{H}_c) / ({}^3\text{H}_c - {}^3\text{H}_b) \quad (2)$$

The calculation is affected by uncertainties related to the estimated discharge  $Q_a$  (in the order of 4–7 % according to Day 1977), and by uncertainties related to the calculated isotopic values (as reported in Table 4). The final uncertainty is assessed by using the common error propagation method, reported in Taylor (1997).

#### Results

##### Water and groundwater chemical and isotopic analyses

The results of chemical and isotopic analyses are presented in Table 2. Water total dissolved solids ranges from 0.11 to

**Fig. 4** Piper diagram. Water samples from the tectonic window of Gova (river network DR and ES, Na–Cl groundwater occurrences GO and Macognano brackish spring BSM, labels are referred to Table 2 while locations are shown in Fig. 3) are reported with shallow springs S1, S2, S3, S4, S5, S6, Poiano evaporites-related spring S7 and Ca' Lita CG and Canalina brackish water BSC (Table 2; Fig. 2)

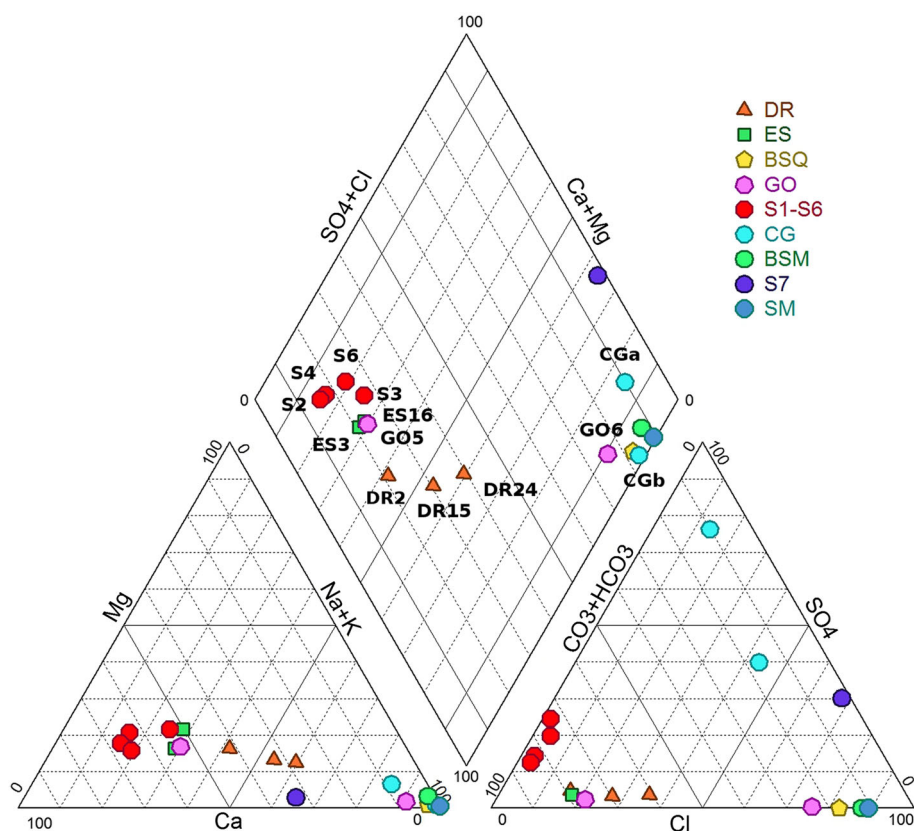
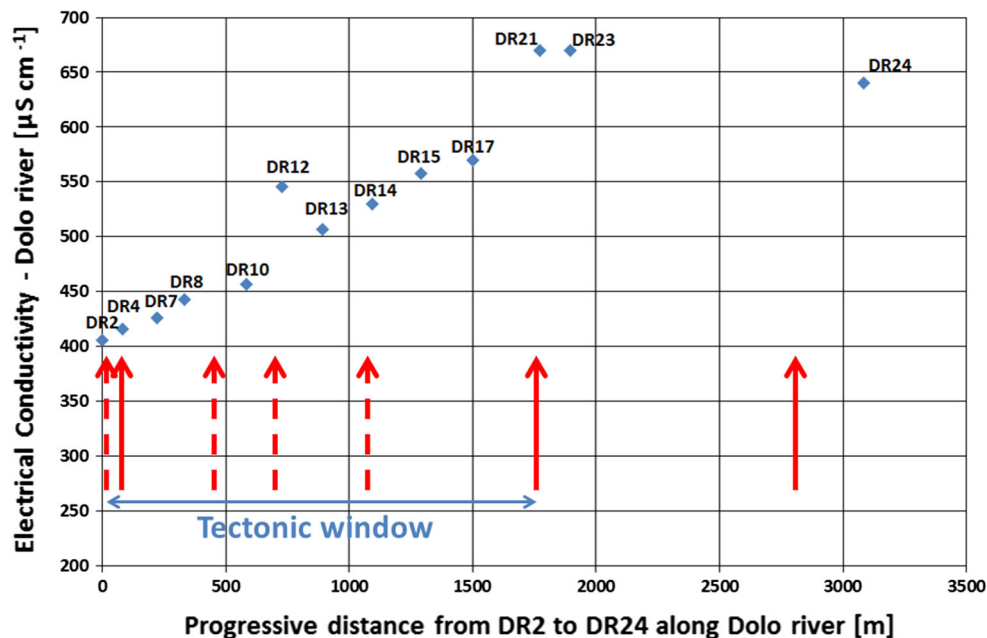


**Fig. 5** Year 2010 electric conductivity profile along the cross-section of Fig. 3 (see Table 2 for the corresponding electric conductivity values). The tectonic window extent (blue arrow) and location of faults (continuous red line) and fractures (dashed red line) as shown in Fig. 3a, b are also reported



$0.17 \text{ g l}^{-1}$  (Lago Verde shallow spring S4; Dolo River at the initiation of tectonic window DR2), up to  $6.6$  and  $8.8 \text{ g l}^{-1}$ . These latter samples were collected from Quara (BSQ) and Macognano (BSM) springs and they can be classified as brackish water. In particular, they are Na–Cl (salinity of  $5.5$  and  $7.6 \text{ g l}^{-1}$ , respectively) water with a not-negligible amount of  $\text{HCO}_3^-$  (up to  $1,200 \text{ mg l}^{-1}$  in BSQ). The value of  $\text{pCO}_2$  is  $4.65 \text{ kPa}$  (BSQa) while both are characterized by supersaturation in carbonates (calcite, aragonite and dolomite).

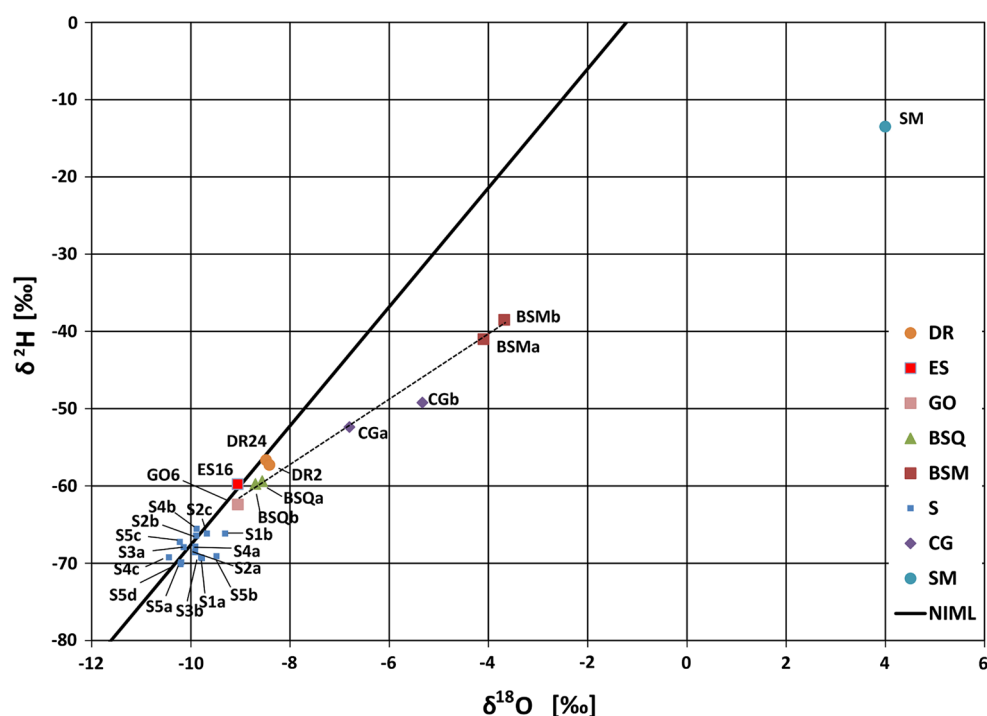
If samples are reported together inside a Piper diagram (Fig. 4), several river water samples collected upstream, at the very beginning of the tectonic window (DR2, ES1, ES3) fall close to the left side of the diamonds, which represents the Ca– $\text{HCO}_3$  hydro-facies corner. This group is normally composed by poorly mineralized shallow groundwater (in our case salinity up to  $0.06 \text{ g l}^{-1}$ , see Table 2) which is related to short-time circuits normally fed by rainfall and snowmelt recharge. Moving downstream, DR15, DR24 river samples and GO5 groundwater occurrence are shifted towards the right part of the diagram, aligned with the Na–Cl hydro-facies (GO6–BSQa). This fact highlights the presence of a mixing process with the Na–Cl end-member, acting progressively down to the termination of the tectonic window, represented by the main normal fault (at the horizontal distance  $1,800 \text{ m}$ , Fig. 5). Inside the tectonic window (blue arrow in Fig. 5), the EC is progressively increasing from  $406$  (DR2) to  $570 \mu\text{S cm}^{-1}$  (DR 17, horizontal distance  $1,500 \text{ m}$ ), if point DR12 is excluded ( $546 \mu\text{S cm}^{-1}$ ), where a not complete homogenization among the two end-members can be inferred, due to the local site conditions along the

riverbed, also considering the values measured at immediately downstream sampling points ( $507$  at DR13 and  $530 \mu\text{S cm}^{-1}$  at DR14) and the overall trend of the EC. Inside the tectonic window, the gradient is in the order of  $11 \mu\text{S cm}^{-1}$  every  $100 \text{ m}$ , whereas from DR17 to DR 21 ( $670 \mu\text{S cm}^{-1}$ ), the gradient is three times greater ( $33 \mu\text{S cm}^{-1}$  every  $100 \text{ m}$ ).

Trace ions show clear anomalies:  $B_{\text{tot}}$  reaches concentrations up to  $28.3 \text{ mg l}^{-1}$  in BSMb. This ion is normally present in  $\mu\text{g l}^{-1}$  in the common groundwater (Toscani et al. 2001; Duchi et al. 2005).

The values of  $\delta^{18}\text{O}$  and  $\delta^2\text{H}$  from superficial water (DR2, DR24, ES16), groundwater occurrences (GO6) and from shallow springs (S1, S2, S3, S4, S5) samples are between  $-10.44$  to  $-8.32 \text{ ‰}$  and  $-70.15$  to  $56.65 \text{ ‰}$ , respectively. Plotting all the collected samples in a  $\delta^{18}\text{O}$ – $\delta^2\text{H}$  graph (Fig. 6), with the exception of Na–Cl water (GO6; BSQa; BSMA; BSMb), they lie on the Northern Italy Meteoric Line (NIML) proposed by Longinelli and Selmo (2003), showing a clear rainfall and snowmelt origin. Moreover, it can be noticed that for most mineralized Na–Cl water GO6 and BSQa, a slight depletion of  $\delta^2\text{H}$  results in a downward shift. In all the cases,  $\delta^{18}\text{O}$  values are highly negative if compared with the isotopic signal which should characterize the mean annual rainfall for this altitude ( $\delta^{18}\text{O}$  ranging from  $-7.9$  to  $-8.2 \text{ ‰}$  for an elevation between  $500$  and  $900 \text{ m a.s.l.}$ , raingauge stations exclusively from the northern Apennines in Longinelli and Selmo 2003). This is consistent with other results recently obtained on springs discharging from flysch and carbonatic units in the northern and central Apennines of Italy (Tazioli et al. 2007; Iacumin et al. 2009; Minissale and Vaselli 2011; Cervi

**Fig. 6** Graph  $\delta^{18}\text{O}$ – $\delta^2\text{H}$ . Some representative samples from the river network, Na–Cl groundwater occurrences, Quara and Macognano and Ca– $\text{HCO}_3$  shallow springs (see Table 2) are plotted together with Salvarola mud volcano (Boschetti et al. 2011), Ca’ Lita brackish water (Cervi et al. 2012). Dashed line represents the alignment of the  $^2\text{H}$  depleted samples in the tectonic window. NIML (Northern Italy meteoric line by Longinelli and Selmo 2003) is also plotted



et al. 2014). The authors have related this behaviour on the one hand with the homogenization effect occurring on the isotopic signal of rainfall inside the aquifers, on the other hand with the incapability of summer rainfall to reach the groundwater because of high evapotranspiration effects (Cervi et al. 2012). Considering the hydrological water balance calculated for the same time-window of the study (section “[Geological and hydrogeological settings](#)”), aquifers recharge is concentrated in the late autumn–beginning of spring period, when rainfall and snowmelt generally provide lighter isotopic values.

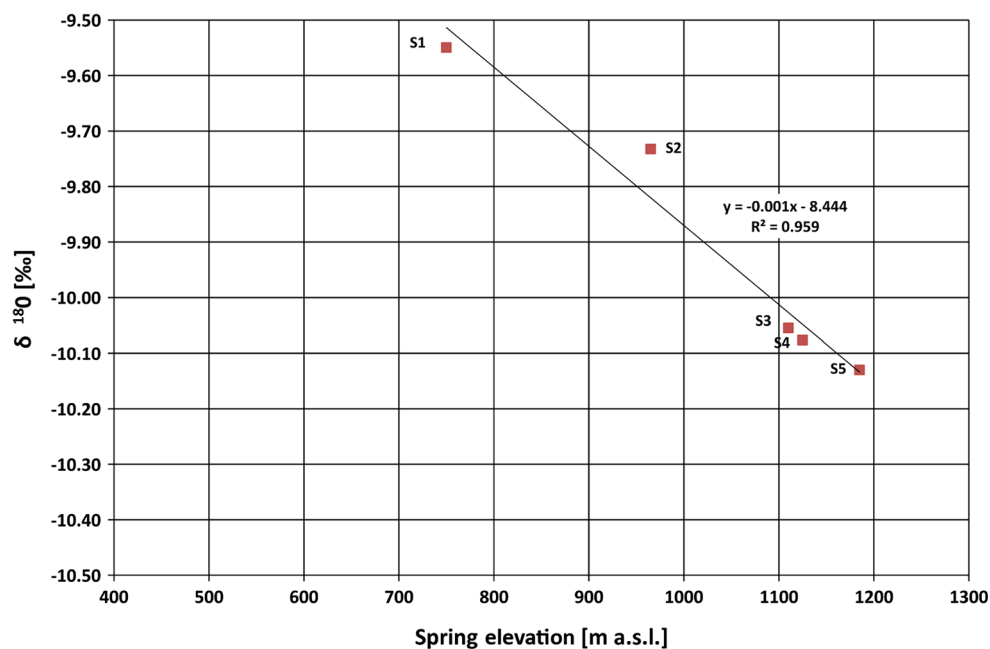
The  $\delta^{18}\text{O}$ –altitude plot (Fig. 7) obtained using shallow springs provides further confirmations; aquifers recharge is characterized by depleted values of  $\delta^{18}\text{O}$ : BSQ and BSM (both characterized by the same elevation of about 500 m a.s.l.) should be characterized by  $\delta^{18}\text{O}$  equal to  $-9.14$  ‰. In the last case (BSMa, BSMb),  $\delta^{18}\text{O}$  values were highly enriched ( $-4.10$  ‰;  $-3.68$  ‰). In the study area, these enriched values are never detected, even in rainfall (Cervi et al. 2012). Moreover, water samples coming from Macognano presented high depletion of  $\delta^2\text{H}$  and can be linked to the other Na–Cl water samples along a line, which displays a lower inclination with respect to that of the meteoric line (Fig. 6). Despite this behaviour is similar to that noticed in residual water undergoing an evaporation process (Mazor 1997; Kendall and McDonnell 1998), this phenomenon can be certainly excluded in this case. First of all, as previously mentioned, the isotopically heaviest summer rainfall doesn’t infiltrate through the soil, as clearly demonstrated by applying the Thornthwaite and

Mather (1957) soil-balance equation. Furthermore, both Quara (BSQa, BSQb) and Macognano (BSMa, BSMb) brackish springs were sampled during two different campaigns and  $\delta^{18}\text{O}$  values are available (see Table 2). As reported by Gonfiantini et al. (1974) and Simpson et al. (1987), evaporation process should lead to positive correlation between salinity and  $\delta^{18}\text{O}$  in the residual water. On the contrary, this is not occurring in both locations, where samples showing the most enriched values of  $\delta^{18}\text{O}$  are characterized by lower electric conductivities.

As reported in Table 2, tritium amounts have been measured in the river at the initiation of the tectonic window (DR2) and 1,000 m downstream of the normal fault (DR24), as well as in BSQa and BSMa. DR2 tritium content was lower than expected (6.3 TU). In particular, in this sector of chain, mean annual rainfall is characterized by weighted values of about 8–9 TU (Tazioli 2011a, b; Cervi et al. 2012). The 6.3 TU value noticed upstream (DR2) can be explained if tritium variability content in rainfall is taken into account. It is well known that precipitations are characterized by high variability in their TU content, with higher values in June and lower values during the Autumn–Winter periods in this sector of mountain chain (Tazioli 2011a, b). Since water was sampled from the river in September, the recent precipitations characterized by lower tritium content eventually fed the superficial network providing the more depleted TU amounts.

Moving downstream, tritium slightly decreased at the end of the tectonic window (DR24 5.8 TU); this seems to be consistent with the progressive mixing between river

**Fig. 7** Graph elevation— $\delta^{18}\text{O}$  and corresponding regression line for Ca– $\text{HCO}_3$  shallow springs (S1, S2, S3, S4, S5; see Table 2). Elevation: S1 750 m a.s.l.; S2 965 m; S3 1,110 m; S4 1,125 m; S5 1,185 m. The isotopic data are reported also in Table 2, and the values are averaged for the period 2005–2008



water (6.3 TU) and highly mineralized water, characterized by low or null value of tritium activity (BSQa 0.7 TU, BSMa 0 TU).

In particular, as highlighted by Clark and Fritz (1997) and Mazor (1997), water with TU < 0.8 proves that its infiltration occurred before the tritium atomic peak in 1952. As such, the tritium values presented here can be considered, once again, a general indicator of mixing between younger recharge water and older water, involved in longer flow-paths.

#### PHREEQC modelling

Results of the simulations are reported in Table 5. Attention has been paid in particular to chlorine and boron, since these elements mostly reflect processes that are not related to changes in the redox state and do not suffer for further reactions of adsorption and exchange (Wedepohl 1969; Walker 1975; Hem 1985; Appelo and Postma 2005). With reference to the first scenario that has been tested (Simulation 1: long-term interaction between rainfall and flysch rock through pores), no chloride and boron were detected in the at-equilibrium water. This is due to the absence of solid phases, which could contain  $\text{Cl}^-$  and  $\text{B}_{\text{tot}}$  and could provide these ions to the final solution. More in detail, active clays such as illite (which is present in the mineralogical assemblage as 5 %) can adsorb very small quantity of boron if peculiar redox conditions take place (Keren and Mezuman 1981); this process is possible in marine environment (Eriksson et al. 1996). Anyway, once boron is adsorbed into the clay minerals and incorporated into the tetrahedral sheet structures, it cannot be released by

exchange processes at low temperature (Couch 1971) as in the case of Simulation 1 ( $t = 20^\circ\text{C}$ ).  $\text{Na}^+$  exceeded  $0.12 \text{ g l}^{-1}$  while  $\text{Ca}^{2+}$  was absent.

Starting from the mineralogical assemblage as reported in Simulation 2 (long-term interaction between sea water and sediments which are involved in burial processes) pore water became progressively enriched in  $\text{Na}^+$  (up to  $414 \text{ g l}^{-1}$ ) through albite dissolution and  $\text{Ca}^{2+}$  ( $9.6 \text{ g l}^{-1}$ ).  $\text{Cl}^-$  peak was found at step 7 (equal to  $176 \text{ g l}^{-1}$ ) when halite phase reached the saturation point and consequently started to precipitate from the solution. At step 10,  $\text{Cl}^-$  decreased down to  $16.8 \text{ g l}^{-1}$ . Due to the presence of marine water and relative higher temperature with respect to Simulation 1, exchange process between pore solution and boron has been taken into account. Starting from step 7,  $\text{B}_{\text{tot}}$  abruptly increased owing its concentration in the solution up to  $231 \text{ g l}^{-1}$ .

In the early stage of sedimentation (step 0), pore water resulted highly supersaturated in chlorite and calcite, which could thus precipitate from the solution. During the burial processes (step from 1 to 10), calcite remained every time saturated. This is in accordance with the secondary cement types found in the Gova sandstones.

#### Discussion

##### Origin of the Na–Cl end-member and mixing processes with Ca– $\text{HCO}_3$ water

The presence of an active mixing process between different water types was clearly detected in the Gova area, starting from the very beginning of the tectonic window. In fact,

**Table 5** Results of the modelling of the long-term interaction between pore water and host rocks performed with the software PHREEQC (chemical composition of the residual pore solution)

Simulation	Step	t (°C)	P (MPa)	Ca <sup>2+</sup> (mg l <sup>-1</sup> )	Na <sup>+</sup> (mg l <sup>-1</sup> )	Cl <sup>-</sup> (mg l <sup>-1</sup> )	B <sub>tot</sub> (mg l <sup>-1</sup> )	SI calcite	SI anhydrite	SI gypsum	SI halite	SI chlorite
1	0	20	0.1	1	4	5	0	-2.0	-3.5	-3.1	-9.2	-9,999
	1	20	0.1	0	129	5.5	0	-1.4	-6.4	-5.9	-7.7	-2.9
2	0	4	0.1	427	11,200	20,100	4.8	1.2	-1	-0.5	-2.4	21.8
	1	17.6	5.3	517	13,900	20,300	4.8	0	-0.8	-0.5	-2.4	-2.9
	2	31.2	10.6	520	13,900	20,300	4.8	0	-0.8	-0.5	-2.4	-3.4
	3	44.8	15.9	524	13,900	20,300	4.8	0	-0.7	-0.6	-2.4	-3.7
	4	58.4	21.2	530	13,900	20,300	4.8	0	-0.6	-0.6	-2.4	-4
	5	72	26.6	537	13,900	20,300	4.8	0	-0.4	-0.6	-2.5	-4.2
	6	85.6	31.9	546	13,900	20,300	4.8	0	-0.3	-0.5	-2.5	-4.3
	7	99.2	37.2	601	118,000	176,000	41.9	0	0	-1.1	-0.3	-8.4
	8	112.8	42.5	2,990	336,000	43,600	12,200	0	0	-1.5	0	-9.6
	9	126.4	47.8	6,330	414,000	23,700	191,000	0	0	-2	0	-10.1
10	140	53.1	9,610	444,000	16,800	231,000	0	0	-2	0	-10.7	

Simulation 1: starting solution was set equal to rainfall (Panettiere et al. 2000). Simulation 2: starting solution was set equal to sea water (Nordstrom et al. 1979). The progressive growth of pressure and temperature was simulated with a step by step procedure until both have reached the maximum values proposed by Carlini et al. (2013)

values of EC measured in the Dolo River increase moving downstream with an almost constant rate and appear not to be influenced by the presence of faults and fractures crossing the valley (Fig. 5).

The mixing process takes place starting from two end-members, which are characterized by evident chemical and isotopic differences. The first hydrofacies is represented by common and poorly mineralized water related to rainfall and snowmelt recharge taking place from November to April. By infiltrating into the slopes, rainfall and snowmelt water feed aquifers, becoming progressively more enriched in Ca and HCO<sub>3</sub> ions, while δ<sup>18</sup>O and δ<sup>2</sup>H isotopic content always lies close to the NIML.

The second hydrofacies is represented by Na–Cl water (salinity up to 7.6 g l<sup>-1</sup> in BSMa), which is strongly enriched in Sr<sup>2+</sup> and B<sub>tot</sub> (up to 11.5 and 28.3 mg l<sup>-1</sup>, respectively; Sr<sup>2+</sup> from Colombetti and Nicolodi 2005; Boschetti et al. 2011). Boron is normally detected in µg l<sup>-1</sup> in common shallow springs of the northern Apennines (in-trace ion), while strontium can vary from 3 to 6 mg l<sup>-1</sup> (as reported by Toscani et al. 2001; Duchi et al. 2005). Behaving in a more conservative way than Sr<sup>2+</sup>, boron can hardly precipitate from the solution (Walker 1975; Grew and Anovitz 1996) and can be considered as a useful marker for unravelling the origin of this hydrofacies. As anticipated beforehand, Mather and Porteous (2001) stressed that the long-term interaction between rainfall water and host rocks (such as flysch rock containing clays) cannot in itself justify the measured B<sub>tot</sub> values. In particular, even considering the presence of evaporites (as supposed by Colombetti and Nicolodi 2005) containing halite such as those outcropping

7 km northward of the Gova area, rainfall and snowmelt recharge cannot anyway provide springs characterized by a B<sub>tot</sub> content of more than 0.1 mg l<sup>-1</sup> (for instance, Poiano spring; Cervi 2003, Table 2).

Water types with similar B<sub>tot</sub> content are those related to Pliocene connate water and deep oilfields, located in the frontal part of the northern Apennines, such as some mud volcanoes (for instance Salvarola: 121 mg l<sup>-1</sup> in Boschetti et al. 2011; Fig. 2; Table 2). Other brackish occurrences are located close to regional faults connected to oilfields only (CGa in Table 2: 8.5 mg l<sup>-1</sup>; Cervi et al. 2012; BSC in Table 2: 16.0 mg l<sup>-1</sup>). Ion Cl<sup>-</sup> is another ion which can hardly precipitate from the solution (Mazor 1997) and can be used, together with B<sub>tot</sub>, in the diagnostic graph proposed by Fontes and Matray (1993) and successively used by Boschetti et al. (2011) for the water of the northern Apennines (Fig. 8). Macognano and Gova (Cl<sup>-</sup> values of 4,634 and 4,059 mg l<sup>-1</sup>, respectively; Colombetti and Nicolodi 2005; Boschetti et al. 2011) are shifted towards Salvarola mud volcano (SM in Table 2 10,190 mg l<sup>-1</sup>; Boschetti et al. 2011) and lie on a line connecting shallow groundwater (represented by S6, Table 2) and oilfield-associated water (CGa in Table 2; Cervi et al. 2012; BSC in Table 2; see also Tassi et al. 2012).

As anticipated in section “Water and groundwater chemical and isotopic analyses”, stable isotopes content shows enrichment in δ<sup>18</sup>O which becomes progressively more positive, up to the value of -3.68 ‰ detected in the Macognano brackish spring (BSMb). By plotting the same water samples in a δ<sup>18</sup>O–B<sub>tot</sub> (Cervi et al. 2012), the mixing behaviour between the two end-members is furthermore confirmed (Fig. 9).

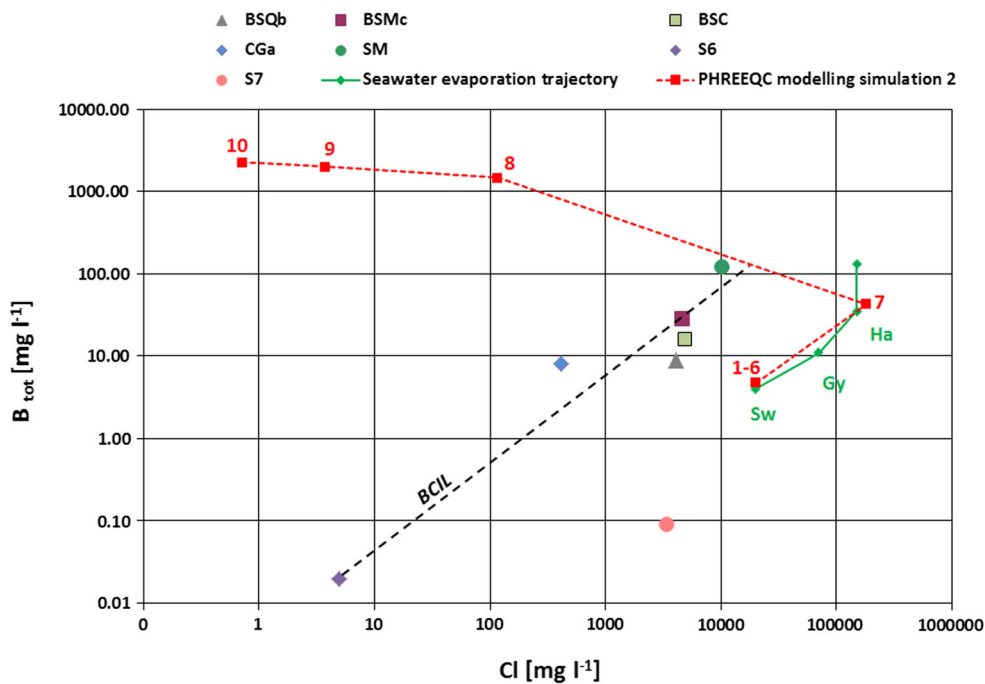
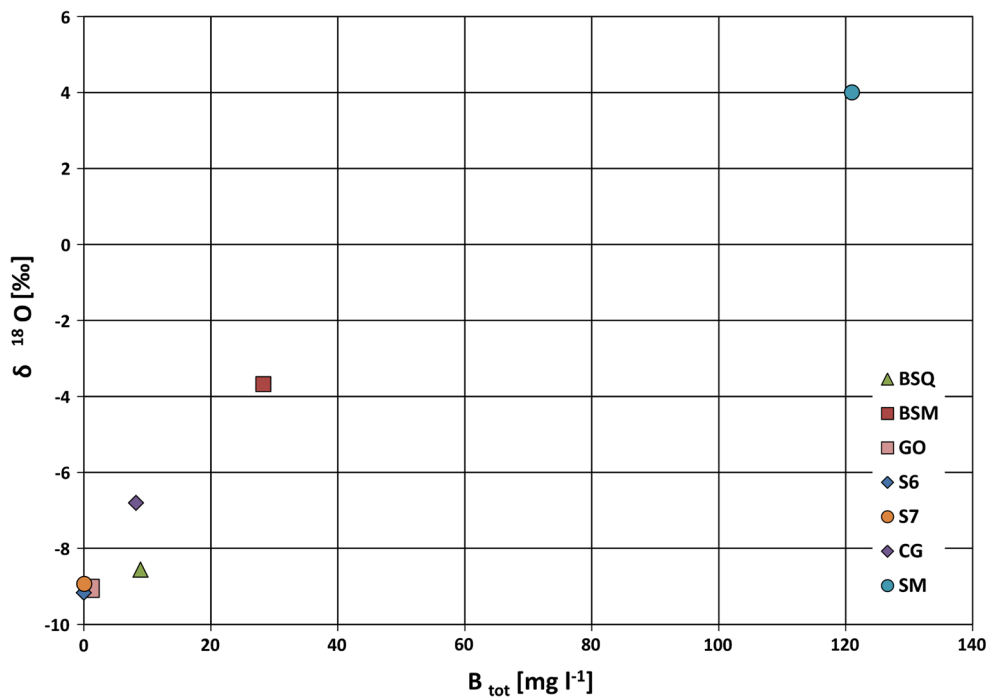


**Fig. 8** Plot  $Cl^- - B_{tot}$ . Some representative samples from the river network, Na–Cl groundwater occurrences, Quara and Macognano and a Ca–HCO<sub>3</sub> shallow spring external to the study area (S6, see Table 2) are plotted together with Salvarola mud volcano (SM; Boschetti et al. 2011), Ca’ Lita and Canalina brackish water (CG; Cervi et al. 2012; BSC; see Table 2) and Poiano evaporites-related

spring (S7; Cervi 2003). *Dashed line* (BCIL) represents the alignment of  $B_{tot}$ -rich Na–Cl water samples. The *red line* represents progressive steps (6–10) of the PHREEQC modelling during Simulation 2 (see Table 5 for temperature and pressure data). The green line represents sea water evaporation trajectory as reported by Fontes and Matray (1993) with gypsum and halite precipitation points

**Fig. 9**  $\delta^{18}O - B$ . Some representative samples from the river network, Na–Cl groundwater occurrence GO, Quara BSQ and Macognano BSQ and a Ca–HCO<sub>3</sub> shallow spring external to the study area (S6, see Table 2) are plotted together with Salvarola mud volcano SM (Boschetti et al. 2011), Ca’ Lita brackish water CG (Cervi et al. 2012) and Poiano evaporites-related spring S7 (Cervi 2003)



The presence of mixing processes is corroborated also by considering isotopic content alone. In fact, following the approach proposed by Gibson et al. (2005), the intersection

between the alignment of Na–Cl water samples and the meteoric waterline can be considered as representative of the amount of  $\delta^{18}O - \delta^2H$  in rainfall and snowmelt recharge

water (Fig. 6). This provides a  $\delta^{18}\text{O}$  value of  $-9.51\text{‰}$ , which is consistent with a mean recharge elevation of about 750 m a.s.l., as calculated by using the shallow springs reported in Table 2 and Fig. 7, i.e. at the mean altitude of the Gova sandstones outcrops in the area. The values found for Macognano BSMa and Quara BSQa ( $-3.68$  and  $-8.70\text{‰}$ , respectively) are less negative, being enriched in the heaviest isotope, implying a mixing with a more positive water end-member. If the water from Salvarola mud volcano SM was considered as possible isotopic marker ( $\delta^{18}\text{O}$  equal to  $+4\text{‰}$ ), a mixing NaCl–CaHCO<sub>3</sub> groundwater in the order of 43–57 % can be estimated for the BMS. This result is in agreement with the simplified chemical equilibrium analysis that was conducted coupling the mineralogical compositions of the Gova sandstones using PHREEQC software in Simulation 2. In Fig. 8, the intercept of the BCIL ( $B_{\text{tot}}\text{--Cl}^-$  intercept line connecting the only groundwater samples Btot-rich BSMc, BSQb, SM, CGa and BSC with the common shallow groundwater from the northern Apennines S6) and the output of the modelling between steps 7 and 8 (temperature between 99 and 112 °C and pressure ranging from 36.7 to 42 MPa) provide the values for  $B_{\text{tot}}$  and  $\text{Cl}^-$  of the Na–Cl end-member (about 150 and 26,000 mg l<sup>-1</sup>, respectively).

The helium content detected by Tassi et al. (2012) in BSM (equal to 0.008 mmolmol<sup>-1</sup>) confirms the presence of an old water and allows the age to be estimated by using the formula proposed by Steiger and Jager (1977) and by considering crustal average uranium and thorium contents equal to 2.8 and 10.7 mg kg<sup>-1</sup>, respectively (Taylor and McLennan 1985), an age of about 2 million years is obtained. This value is between those (1.6–3.3 million years) which can be calculated taking into account the mean Italian flysch rock mass composition (uranium and thorium equal to 1.8–3.2 and 0.5–3.1 mg kg<sup>-1</sup>, respectively; Tositti and Sogni 2007). Then, if the mixing proportion from the two end-members was considered (again, 43 and 57 %), an age in the range of 3.8 and 7.8 million years can be estimated. Being the age of burial dated back to the Early Miocene (16–20 million years), this apparent discrepancy could be explained considering the equilibration process taking place between rising He-rich gases and the atmosphere.

The results of EC measurements, of chemical and isotopic analyses and of modelling are consistent with a rainfall and snowmelt recharge water leaching an oilfield reservoir hosted within the sandstone unit. In particular, the simulations confirmed the importance of sea water and burial processes for the development of the Na–Cl facies, which originated directly within the Gova sandstones and do not have an external and deeper origin.

A diffuse flow from the network of mesostructures is demonstrated by the trend of the EC value, which is

linearly increasing along the river flowing in the tectonic window. The peak of EC at the very end of the tectonic window is related to the geological and structural setting: here the salt water flow-paths are confined from the outcropping of almost impermeable clayey rock masses.

#### Assessment of the Na–Cl inflow through the tectonic window

The amount of Na–Cl water inflow into the river streambed was estimated by using the isotopic balance approach described in section “Hydrological water balance”. Table 4 summarizes relevant data and results. By applying the dilution salt method described in section “Field surveys: water sampling and physical parameters assessment, river discharge assessment” at the beginning of the tectonic window, river discharge ( $Q_a$ ) was estimated in the order of  $150 \pm 6 \text{ l s}^{-1}$ . Tritium content related to the Na–Cl water aliquot ( $H_b$ ) was equal to 0.0 TU, while  $H_a$  was 6.3 TU. The final amount of highly mineralized Na–Cl water ( $Q_b$ ) can be estimated in about  $12.9 \pm 5.9 \text{ l s}^{-1}$ . This value seems to be rather high if compared to the Chloride contents of the water samples linked to the corresponding discharges  $Q_a$ ,  $Q_b$ ,  $Q_c$ . In fact, by considering  $\text{Cl}_a^-$ ,  $\text{Cl}_b^-$  and  $\text{Cl}_c^-$  instead of  $^3\text{Ha}$ ,  $^3\text{Hb}$  and  $^3\text{Hc}$  in Eq. (2), and so equal to 23, 4,634 and 78 mg l<sup>-1</sup> (see DR2, BSMc and DR24 in Table 2), an hypothetical  $Q_b$  should be in the order of  $1.7 \pm 0.4 \text{ l s}^{-1}$ . As discussed in section “Water and groundwater chemical and isotopic analyses”, highly mineralized water flowing out from flysch bedrock showed different degree of mixing with rainfall and snowmelt water; therefore, final water samples are characterized by a variable range of salinity, even when displaying very low values of tritium activity (see, for example, BSQa in Table 2: 0.7 TU). This could be due to the time taken for rainfall and snowmelts water to follow long flow-paths, during which tritium content is halved every 12.3 years (Mazor 1997). This process can result in water with highly variable salinity but similar TU (Table 2; DR2, DR24, BSQa, BSMa).

#### Conclusions

In the tectonic windows of the northern Apennines, Na–Cl water types can be found frequently. The Gova tectonic window is an ideal test-site to understand the mixing processes between shallow Ca–HCO<sub>3</sub> and deep Na–Cl groundwater in this geological setting. In fact, its relatively small dimensions and simple geological structure, together with a poorly developed drainage network, facilitate investigation and monitoring activities in the frame of an original and comprehensive hydrogeological study. The

results have allowed the characterization of the origin and the assessment of the deep-water aliquot.

The study consisted of hydrological, hydrochemical and isotopic surveys which were carried out on superficial water and on groundwater samples collected during summer 2010 along the tectonic window of Gova, and from the brackish and shallow springs flowing out from the surrounding slopes during the period 2005–2012. The water and groundwater chemistry and the stable isotope contents were estimated in order to characterize end-members origin and mixing phenomena. By collecting local springs water, the reference isotopic values ( $\delta^{18}\text{O}$ ) for rainfall recharge water were defined and linked to the estimated infiltration through the Gova flysch rock mass.

The aliquot of deep Na–Cl water was estimated by coupling radioactive isotopes content ( $^3\text{H}$ ) with river discharge in the southern sector of the tectonic window. The study was conducted during a period of minimum discharge in the Dolo River, in order to enhance the contribution of the Na–Cl water into the streambed and to reduce the errors in the calculation of the corresponding aliquot.

An independent validation, to check if the peculiar water chemistry could be due only to the mineralogical composition of the Gova flysch rocks, consisted in a PHREEQC equilibrium-based model that took into account the long-term chemical interaction between pore water solutions and host rocks.

Results confirmed the presence of old Na–Cl water with salinity increasing up to  $5.5 \text{ g l}^{-1}$  at the northern termination of the tectonic window. These latter values are in agreement with the ions contents of the most mineralized spring (Macognano brackish spring: salinity of  $7.6 \text{ g l}^{-1}$ ), which has been considered as having the deepest and longest flow-path. Stable isotopes and trace ions contents are consistent with a rainfall and snowmelt recharge leaching an oilfield reservoir hosted at depth. The simulations confirmed the importance of sea water and burial processes for the development of the Na–Cl facies. Considering as end-member the Na–Cl water, a cumulate inflow in the range of  $12.9 \pm 5.9 \text{ l s}^{-1}$  has been estimated, i.e. in the order of the 10 % of the river discharge. This aliquot is released into the river network with different mixing proportion by groundwater occurrences flowing out from the autochthonous flysch unit.

## References

- Alberti LB (1552) Descrizione di tutta Italia  
 Analisi preliminare per la valutazione del potenziale geotermico in Emilia-Romagna. <http://ambiente.regione.emilia-romagna.it/geologia/temi/geotermia/analisi-preliminare-valutazione-potenziale-geotermico-emilia-romagna-rapporto-2010>. Accessed 6 February 2013
- APAT (2002) Carta Geologica d'Italia alla scala 1:50.000—Tav. 235. SELCA, Genova
- Appelo CAJ, Postma D (2005) Geochemistry, groundwater and pollution, 2nd edn. CRC Press, Boca Raton
- Bacci A (1571) De thermis Andreae Baccij Elpidiani, medici, atque philosophi, ciuis Romani, libri septem. Valigrisi, Venezia
- Bertolini G, Gorgoni C (2001) La lavina di Roncovetro (Vedriano, Comune di Canossa, Provincia di Reggio Emilia). *Quaderni di Geologia Applicata* 8:1–21
- Bianchelli M (1553) De distinctione balneorum mineralium. Venezia
- Biondi F (1527) L'Italia illustrata, Basilea
- Boccaletti M, Elter P, Guazzone G (1971) Plate tectonics models for the development of the Western Alps and northern Apennines. *Nature* 234:108–111
- Bonini M (2007) Interrelations of mud volcanism, fluid venting, and thrust-anticline folding: examples from the external northern Apennines (Emilia-Romagna, Italy). *J Geophys Res* 112:1–21
- Bonini M (2013) Fluid seepage variability across the external Northern Apennines (Italy): structural controls with seismotectonic and geodynamic implications. *Tectonophysics* 590:151–174
- Boschetti T, Toscani L, Shouakar-Stash O, Iacumin P, Venturelli G, Mucchino C, Frappe SK (2011) Salt waters of the Northern Apennine Foredeep Basin (Italy): origin and evolution. *Aquat Geochem* 17:71–108
- Botti F, Aldega L, Corrado S (2004) Sedimentary and tectonic burial evolution of the Northern Apennines in the Modena-Bologna area: constraints from combined stratigraphic, structural, organic matter and clay mineral data of Neogene thrust-top basins. *Geodin Acta* 17:185–203
- Buttinelli M, Procesi M, Cantucci B, Quattrocchi F, Boschi E (2011) The geodatabase of caprock quality and deep saline aquifers distribution for geological storage of  $\text{CO}_2$  in Italy. *Energy* 36:2968–2983
- Camerana E, Galdi B (1911) I giacimenti petroliferi dell'Emilia; Carte e Sezioni geologiche. *J Geophys Res* 97(13):917–951
- Capozzi R, Picotti V (2002) Fluid migration and origin of a mud volcano in the Northern Apennines (Italy): role of deeply rooted normal fault. *Terra Nova* 14(5):363–370
- Capozzi R, Picotti V (2010) Spontaneous fluid emission in the northern Apennines: geochemistry, structures, and implications for the petroleum system. *Geol Soc Spec Publ* 348:115–135
- Carlini M, Artoni A, Aldega L, Balestrieri ML, Corrado S, Vescovi P, Bernini M, Torelli L (2013) Uplift and reshaping of far-travelled/allochthonous tectonic units in mountain belts. New insights for the relationships between shortening and coeval extension in the western Northern Apennines (Italy). *Tectonophysics* 608:267–287
- Cervi F (2003) Idrologia chimica, isotopica e radiometrica dell'alta Val di Secchia (Chemical, isotopic and radiometrical hydrology of the Upper Secchia Valley), BSc Dissertation, Università di Modena e Reggio Emilia
- Cervi F, Ronchetti F, Martinelli G, Bogaard TA, Corsini A (2012) Origin and assessment of deep groundwater inflow in the Ca' Lita landslide using hydrochemistry and in situ monitoring. *Hydrol Earth Syst Sc* 16:4205–4221
- Cervi F, Corsini A, Doveri M, Mussi M, Ronchetti F, Tazioli A (2014) Characterizing the recharge of fractured aquifers: a case study in a flysch rock mass of the northern Apennines (Italy). Accepted in Proceeding of the International Congress on Engineering Geology, Torino
- Ciancabilla N, Ditta M, Italiano F, Martinelli G (2007) The Porretta thermal springs (Northern Apennines): seismogenic structures and long-term geochemical monitoring. *Ann Geophys* 50(4):513–526
- Clark I, Fritz P (1997) Environmental isotopes in hydrogeology. CRC Press Lewis Publishers, Boca Raton

- Colombetti A, Nicolodi F (2005) Le sorgenti a bassa termalità di Quara (Comune di Toano—Provincia di Reggio Emilia). *Geologia dell'Ambiente Anno XIII* 1:12–16
- Corsini A, Cervi F, Ronchetti F (2009) Weight of evidence and artificial neural networks for potential groundwater spring mapping: an application to the Mt. Modino area (Northern Apennines, Italy). *Geomorphology* 111(1–2):79–87
- Couch EL (1971) Calculation of palaeosalinities from boron and clay mineral data. *Bull Am Assoc Pet Geol* 55:1829–1837
- Crevaschi F (2008) Evidenze isotopiche, chimico-fisiche e piezometriche della circolazione idrica sotterranea in acquiferi fratturati e porosi dell'Appennino settentrionale (Monte Modino, Alta Val Secchia) (Isotopical, chemical and piezometric evidences of groundwater circulation through fractured and porous aquifers of the northern Apennines), BSc Dissertation, Università di Modena e Reggio Emilia
- Day TJ (1976) On the precision of salt dilution gauging. *J Hydrol* 31:293–306
- Day TJ (1977) Observed mixing lengths in mountain streams. *J Hydrol* 36:125–136
- Duchi V, Venturelli G, Boccasavia I, Bonicolini F, Ferrari C, Poli D (2005) Studio geochimico dei fluidi dell'Appennino Tosco-Emiliano-Romagnolo. *Boll Soc Geol It* 124:475–491
- Eriksson A, Reczko BFF, Piper DP (1996) An interpretation of boron contents within Palaeoproterozoic volcano-sedimentary succession: Pretoria Group, Transvaal Supergroup, South Africa. *Precambrian Res* 78:273–287
- Fontes JC, Matray JM (1993) Geochemistry and origin of formation brines from the Paris Basin, France. Part 1: brines associated with Triassic salts. *Chem Geol* 109:149–175
- Freeze RA, Cherry JA (1979) *Groundwater*. Prentice-Hall, Englewood Cliffs
- Gao XB, Wang YX, Wu PL, Guo QH (2010) Trace elements and environmental isotopes as tracers of surface water-groundwater interaction: a case study at Xin'an karst water system, Shanxi Province, Northern China. *Environmental Earth Sciences* 59(6):1223–1234
- Gibson JJ, Edwards TWD, Birks SJ, St Amour NA, Buhay WM, McEachern P, Wolfe BB, Peters DL (2005) Progress in isotope tracer hydrology in Canada. *Hydrol Process* 19:303–327
- Gonfiantini R, Dincer T, Derekoy AM (1974) Environmental isotope hydrology in the Honda region, Algeria. *Isotope Techniques in Groundwater Hydrology IAEA Vienna* 1:293–316
- Gran G (1952) Determination of the equivalence point in the potentiometric titrations. *Analyst* 77:661–671
- Grew ES, Anovitz LM (1996) Boron: mineralogy, petrology and geochemistry. *Rev Mineral* 33:1–864
- Guo QH, Wang YX, Liu W (2010) O, H, and Sr isotope evidences of mixing processes in two geothermal fluid reservoirs at Yangbajing, Tibet, China. *Environmental Earth Sciences* 59(7):1589–1597
- Hem JD (1985) Study and interpretation of the chemical characteristics of natural water. US Geological Survey, Water Supply Paper 2254
- Iacumin P, Venturelli G, Selmo E (2009) Isotopic features of rivers and groundwater of the Parma Province (northern Italy) and their relationships with precipitation. *J Geochem Explor* 102:56–62
- Johnson RH, DeWitt E, Wirt L, Manning AH, Hunt AG (2012) Using geochemistry to identify the source of groundwater to Montezuma Well, a natural spring in Central Arizona, USA: part 2. *Environ Earth Sci* 67(6):1837–1853
- Katsanou K, Siavalas G, Lambrakis N (2012) The thermal and mineral springs of Aitolokarnania Prefecture: function mechanism and origin of groundwater. *Environ Earth Sci* 65(8):2351–2364
- Kebede S, Travi Y, Stadler S (2010) Groundwaters of the Central Ethiopian Rift: diagnostic trends in trace elements,  $\delta^{18}\text{O}$  and major elements. *Environ Earth Sci* 61(8):1641–1655
- Kendall C, McDonnell JJ (1998) *Isotope tracers in catchment hydrology*. Elsevier Sciences, Amsterdam
- Keren R, Mezuman U (1981) Boron adsorption by clay minerals using phenomenological equation. *Clays Clay Miner* 29(3):198–204
- Kligfield R (1979) The northern Apennines as a collisional orogeny. *Am J Sci* 279:676–691
- Kopf AJ (2002) Significance of mud volcanism. *Rev Geophys* 40(2):1005
- Longinelli A, Selmo E (2003) Isotopic composition of precipitation in Italy: a first overall map. *J Hydrol* 270:75–88
- Martinelli Etiope G (2009) “Pieve Santo Stefano” is not a mud volcano: comment on “Structural controls on a carbon dioxide-driven mud volcano field in the Northern Apennines” (by Bonini 2009). *J Struct Geol* 31(10):1270–1271
- Martinelli G, Judd A (2004) Mud volcanoes of Italy. *Geol J* 39:49–61
- Mather J, Porteous NC (2001) The geochemistry of boron and its isotopes in groundwaters from marine and non-marine sandstone aquifers. *Appl Geochem* 16:821–834
- Mazor E (1997) *Chemical and isotopic groundwater hydrology*. Marcel Dekker Inc., New York
- Minissale A, Vaselli O (2011) Karst springs as “natural” pluviometers: constraints on the isotopic composition of rainfall in the Apennines of central Italy. *Appl Geochem* 26(5):838–852
- Minissale A, Magro G, Martinelli G, Vaselli O, Tassi F (2000) Fluid geochemical transect in the northern Apennines (Central-Northern Italy): fluid genesis and migration and tectonic implications. *Tectonophysics* 319:199–222
- Molli G (2008) Northern Apennine-Corsica orogenic system: an update overview. *Geol Soc Spec Publ* 298:413–442
- Nordstrom DK, Plummer LN, Wigley TML, Wolery TJ, Ball JW, Jenne EA, Bassett RL, Crerar DA, Florence TM, Fritz B, Hoffman M, Holdren GR Jr, Lafon GM, Mattigod SV, McDuff RE, Morel F, Reddy MM, Sposito G, Thraillkill J (1979) A comparison of computerized chemical models for equilibrium calculations in aqueous systems. In: Jenne EA (ed) *Chemical modeling in aqueous systems American chemical society symposium Series vol 93*. American Chemical Society, Washington D.C., pp 857–892
- Odeh T, Geyer S, Rödiger T, Siebert C, Schirmer M (2013) Groundwater chemistry of strike slip faulted aquifers: the case study of Wadi Zerka Ma'in aquifers, north east of the Dead Sea. *Environ Earth Sci* 70(1):393–406
- Panettiere P, Cortecchi G, Dinelli E, Bencini A, Guidi M (2000) Chemistry and sulfur isotopic composition of precipitation at Bologna, Italy. *Applied Geochemistry* 15(10):1455–1467
- Parkhurst DL, Appelo CAJ (1999) User's guide to PHREEQC (version 2)—A computer program for speciation, batch reaction, one-dimensional transport and inverse geochemical calculations. *Water Resources Investigations Report 95-4259*, US Geological Survey
- Petitta M, Primavera P, Tuccimei P, Aravena R (2011) Interaction between deep and shallow groundwater systems in areas affected by Quaternary tectonics (Central Italy): a geochemical and isotope approach. *Environ Earth Sci* 63(1):11–30
- Plesi G (2002) Note Illustrative della Carta Geologica d'Italia alla scala 1:50.000, foglio 235 “Pievepelago”. Servizio Geologico d'Italia-Regione Emilia Romagna, Roma Pliny the Elder (77–78 A.D.). *Historia mundi naturalis*, II
- Rantz SE et al (1982) Measurement and computation of streamflow: Volume 1. Measurement of stage and discharge. US Geological Survey Water Supply Paper 2175 Regione Emilia-Romagna (2010)

- Remitti F, Bettelli G, Panini F, Carlini M, Vannucchi P (2012) Deformation, fluid flow, and mass transfer in the forearc of convergent margins: A two day field trip in an ancient and exhumed erosive convergent margin in the Northern Apennines. In: Vannucchi P, Fisher D (eds) *Field guide. Deformation, fluid flow, and mass transfer in the Forearc of Convergent Margins: field guides to the Northern Apennines and in the Apuan Alps*. The Geological Society of America and London, New York, pp 1–34
- Ricci L (1788) *Corografia dei territori di Modena, Reggio e degli altri stati appartenenti alla casa d'Este*. Modena
- Savonarola M (1442) *De balneis e thermis*. Libellus XXII De balneis de aquario. Venezia
- Simpson HJ, Hamza MS, White JWC, Nada A, Awad MA (1987) Evaporative enrichment of deuterium and delta18O in arid zone irrigation. *Isotopes techniques in Water Resources Development*, IAEA Symposium, 299, Vienna: 241–256
- Steiger RH, Jager E (1977) Subcommission on Geochronology: convention on the use of decay constants in gas and cosmochronology. *Earth Planet Sci Lett* 36:359–362
- Tassi F, Bonini M, Montegrossi G, Capecchiacci F, Capaccioni B, Vaselli O (2012) Origin of light hydrocarbons in gases from mud volcanoes and CH<sub>4</sub>-rich emissions. *Chemical Geology* 294–295:113–126
- Taylor JR (1997) *An introduction to error analysis: the study of uncertainties in physical measurements*. University Science Books, Sausalito
- Taylor SR, McLennan SM (1985) *The continental crust: its composition and evolution*. Blackwell, London
- Tazioli A (2011a) Experimental methods for river discharge measurements: comparison among tracers and current meter. *Hydrol Sci J* 56(7):1314–1324
- Tazioli A (2011b) Landfill investigation using tritium and isotopes as pollution tracers. *Aqua Mundi* 1:83–91
- Tazioli A, Tazioli GS (2005) Water and leachate tritium content as pollution tracer in sanitary landfill investigations. In: 10th Int. Waste Management and Landfill Symposium Sardinia 2005, S. Margherita di Pula (CA), CISA
- Tazioli A, Mosca M, Tazioli GS (2007) Location of recharge area of Gorgovivo Spring: a contribution from isotope hydrology. *Int Congr On Isotope Hydrology, IHS-2007 IAEA CN 151(2):27–34*
- Theodorsson P (1999) A review of low-level tritium systems and sensitivity requirements. *Appl Radiat Isot* 50(2):311–316
- Thornthwaite CW, Mather JR (1957) *Instruction and tables for computing potential evapotranspiration and the water balance*. *Publ Clim Drexel Inst Technol* 10:185–311
- Toscani L, Venturelli G, Boschetti T (2001) Sulphide-bearing waters in northern Apennines, Italy: general features and water-rock interaction. *Aquat Geochem* 7:195–216
- Tositti L, Sogni R (2007) La radioattività nelle rocce della regione Emilia—Romagna. In: Angelini P, Gaidolfi L (Eds) *Il radon ambientale in Emilia—Romagna. Prevenzione nei luoghi di vita e lavoro*, Regione Emilia Romagna 51:41–49
- Vallisneri A (1703) *Viaggio per i monti di Modena*. Il volume dell'Opera Omnia: opere fisico-mediche, Venezia
- Valloni R, Cipriani N, Morelli C (2002) Petrostratigraphic Record of the Apennine Foredeep Basins, Italy. *Boll. Soc. Geol. It. Volume speciale* 1:455–465
- Walker CT (1975) *Geochemistry of Boron*. Dowden, Hutchinson & Ross, Benchmark Papers in Geology, Stroudsburg, PA
- Wedepohl KH (1969) *Handbook of geochemistry*. Springer, Berlin